

Subdwarf B stars as possible surviving companions in Type Ia supernova remnants

Xiangcun. Meng^{1,2,3} \star , Jiao. Li^{1,2,4}

¹ Yunnan Observatories, Chinese Academy of Sciences, 650216 Kunming, PR China

² Key Laboratory for the Structure and Evolution of Celestial Objects, Chinese Academy of Sciences, 650216 Kunming, PR China

³ Center for Astronomical Mega-Science, Chinese Academy of Sciences, 20A Datun Road, Chaoyang District, Beijing, 100012, P. R. China

⁴ University of Chinese Academy of Sciences, Beijing 100049, China

ABSTRACT

Although type Ia supernovae (SNe Ia) are so important in many astrophysical fields, a debate on their progenitor model is still endless. Searching the surviving companion in a supernova remnant (SNR) may distinguish different progenitor models, since a companion still exists in the remnant for the single-degenerate (SD) model, but does not for the double degenerate (DD) model. However, some recent surveys do not discover the surviving companions in the remnant of SN 1006 and Kepler's supernova, which seems to disfavor the SD model. Such a result could be derived from an incorrect survey target. Here, based on the common-envelope wind SD model for SNe Ia, in which the initial binary system consists of a white dwarf (WD) and a main-sequence (MS) star, we found that the companion at the moment of supernova explosion may be a MS, red-giant (RG) or subdwarf B (sdB) star if a spin-down timescale of less than 10^7 yr is assumed. We show the properties of the companions at the moment of supernova explosion, which are key clues to search the surviving companions in SNRs. Here, we suggest that the sdB star may be the surviving companion in some SNRs, even if the progenitor systems are the WD + MS systems. The SNe Ia with the sdB companions may contribute to all SNe Ia as much as 22%.

Key words: supernovae: general - white dwarfs - ISM: supernova remnants

1 INTRODUCTION

Although Type Ia supernovae (SNe Ia) are so important in astrophysical fields, e.g. as the best distance indicator to measure the cosmological parameters (Riess et al. 1998; Perlmutter et al. 1999; Meng et al. 2015), what their progenitors are is still an open problem (Hillebrandt & Niemeyer 2000; Leibundgut 2000). Now, it is widely believed that a SN Ia arises from a binary system with at least one carbon oxygen white dwarf (CO WD) (Nugent et al. 2011; Wang & Han 2012; Maoz, Mannucci & Nelemans 2014). The companion of the CO WD may be a normal star, i.e. a main-sequence or a slightly evolved star (WD+MS), a red giant star (WD+RG) or a helium star (WD + He star) (i.e. the single degenerate, SD, model, Whelan & Iben 1973; Nomoto, Thielemann & Yokoi 1984), or another CO WD involving the merger of two CO WDs (i.e. the double degenerate, DD, model, Iben & Tutukov 1984; Webbink 1984). At present, both the SD and the DD models get supports from observations, but also meet problems on the observational and theoretical side.

A basic way to distinguish the different models is to search the surviving companion star in a supernova remnant (SNR), since the SD model predicts that the companion still exists in the SNR,

\star E-mail: xiangcunmeng@ynao.ac.cn

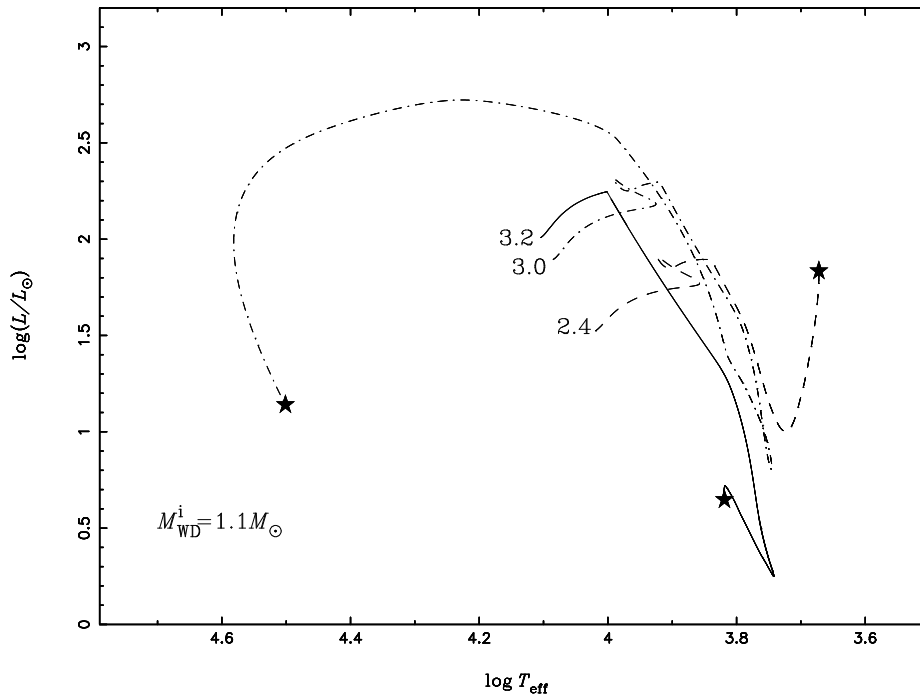


Figure 1. Three examples on the evolution of the companions in HR diagram, where the initial WD mass $M_{\text{WD}}^i = 1.1M_{\odot}$, and the initial periods and the initial companion masses are $[\log(P^i/d, M_2^i/M_{\odot})] = (3.2, 0.2)$, $(3.0, 0.5)$ and $(2.4, 0.5)$, respectively. The asterisks denote the position for supernova explosion.

but does not for the DD model (but see Shen et al. 2018). The discovery of some potential surviving companions in some SNRs shows the power of the method (Ruiz-Lapuente et al. 2004; Li et al. 2017). However, many teams also present negative reports for searching the surviving companions in other SNRs, e.g. in the two famous Galactic SNRs for SN 1006 and Kepler’s supernova, which seems to favor the DD model (González Hernández et al. 2012; Schaefer & Pagnotta 2012; Ruiz-Lapuente et al. 2018; Kerzendorf et al. 2017). A possible solution for this embarrassment of the SD model is from the so-called spin-up/spin-down model, in which the WD is spun up by accretion, and the rapidly rotating WD experience a long spin-down phase before supernova explosion. For the long spin-down timescale, the companion becomes too dim to be detected (Justham 2011; Di Stefano & Kilic 2012; Benvenuto et al. 2015). Before supernova explosion, the companion is usually proposed to become a low-mass helium WD (Justham 2011; Di Stefano & Kilic 2012; Nomoto & Leung 2018), but such a suggestion was not confirmed by searching the surviving WD companion in the remnant of SN 1006 (Kerzendorf et al. 2017). One possible reason is from the huge uncertainty of the spin-down timescale (Di Stefano et al. 2011; Meng & Podsiadlowski 2013). Another possible solution is from the WD + He star channel, where the surviving companion is a very luminous helium star, rather than a dim WD (Wang & Han 2009; McCully et al. 2014), but such a scenario was not confirmed by numerical simulations and observations for SN 1006 (Pan et al. 2014; Kerzendorf et al. 2012; González Hernández et al. 2012). Similarly, no MS or RG stars in the remnant of Kepler’s supernova is suitable to be the surviving companion (Ruiz-Lapuente et al. 2018). However, could there be a possibility that the surviving companion is neither a MS, a RG, a WD, nor a luminous helium star? In this paper, we will investigate this possibility in details.

In section 2, we describe our methods and present the calculation results in section 3. We show discussions and our main conclusions in section 4.

2 METHOD

Recently, Meng & Podsiadlowski (2017) developed a new version of the SD model, i.e. the common-envelope wind (CEW) model which is completely different from the optically thick wind (OTW) model in physics (Hachisu et al. 1996). In the model, a CO WD accretes hydrogen-rich material from its companion to increase its mass, where the companion fills its Roche lobe on the MS or in the Hertzsprung gap (HG). If the mass-transfer rate between the CO WD and the companion exceeds a critical accretion rate, a common envelope (CE) is assumed to form, rather than the onset of the OTW. Within a very wide parameter range, the binary system in the CE may avoid merging and lead to a SN Ia explosion finally, where the SN Ia may explode in the CE phase, in a phase of stable hydrogen burning or a phase of weakly unstable hydrogen burning. At present, the CEW model is still under development, and some parameters used in the present model are relatively conservative, e.g. the CE density is set to be the average density of the CE by assuming a spherical CE structure, and the mass-loss rate from the CE surface is obtained by modifying the Reimers wind formula (Reimers 1975). However, the CE model is quite robust and the CEW model is held within a rather large parameter region (see the detailed discussions in Meng & Podsiadlowski 2017).

The WD may obtain a part of the angular momentum of the accreted material and then rapidly rotate. Since a rapidly rotating WD may not explode even if its mass exceeds $1.378 M_{\odot}$ (Nomoto, Thielemann & Yoon 1984; Yoon, Langer & Scheithauer 2004; Yoon & Langer 2005), we continue our calculations assuming the same WD growth pattern as $M_{\text{WD}} < 1.378 M_{\odot}$, since it is not clear how the WD increase its mass (even not clear whether the WD may continue to increase its mass) after the time of $M_{\text{WD}} = 1.378 M_{\odot}$. To explode as a SN Ia, the rapidly rotating WD must experience a spin-down phase (Justham 2011; Di Stefano & Kilic 2012), which is very crucial to show the signature predicted from a single-degenerate system (Meng & Han 2018). At present, the spin-down timescale is quite uncertain in theory (Di Stefano & Kilic 2012). Based on a fact that circumstellar material (CSM) exists around some SNe Ia, Meng & Podsiadlowski (2013) provide a constraint on the spin-down timescale via a semi-empirical method and they found that the spin-down timescale should be shorter than a few 10^7 yr, otherwise it would be impossible to detect the signature of the CSM. Then, the spin-down timescale probably between 10^5 yr and a few 10^7 yr (Di Stefano & Kilic 2012; Meng & Podsiadlowski 2013). However, when is the time of the onset of the spin-down phase is also uncertain. Here, we assume that the WD explodes as a SN Ia 10^7 yr after the WD grows to $M_{\text{WD}} = 1.378 M_{\odot}$. Such a timescale may be longer than a real spin-down timescale by a few 10^6 yr, i.e. the real spin-down timescale for the WD is less than 10^7 yr while is several times longer than 10^6 yr, which is consistent with the empirical constraints (Meng & Podsiadlowski 2013, 2018). We will discuss the effect of the assumed spin-down timescale on our results in section 4.1. We then record the parameters of the companion at the time of supernova explosion, e.g. the effective temperature, luminosity, mass, radius, binary period and so on.

Since a hybrid carbon-oxygen-neon WD could produce some special SNe Ia, here, we assume that an initial WD leading to SNe Ia may be as massive as $1.3 M_{\odot}$ (Chen et al. 2014; Meng & Podsiadlowski 2014, 2018). We then calculate a dense model grid with different initial WD masses, different initial companion masses and different initial periods. The initial masses of donor stars, M_2^i , range from 2.2 to $4.0 M_{\odot}$; the initial masses of the WDs, M_{WD}^i , from 0.8 to $1.30 M_{\odot}$; the initial orbital periods of binary systems, P^i , from $\log(P^i/\text{day}) = 0.2$ to ~ 15 day, at which the companion star fills its Roche lobe at the end of the HG. The parameter ranges here are smaller than those in Meng & Podsiadlowski (2017, 2018), since in the other ranges, the companions appear as MS or RG stars at the moment of supernova explosion, while we focus on a new kind of surviving companions that no one has mentioned before.

To investigate the birth rate of SNe Ia with special companions, we performed two binary-

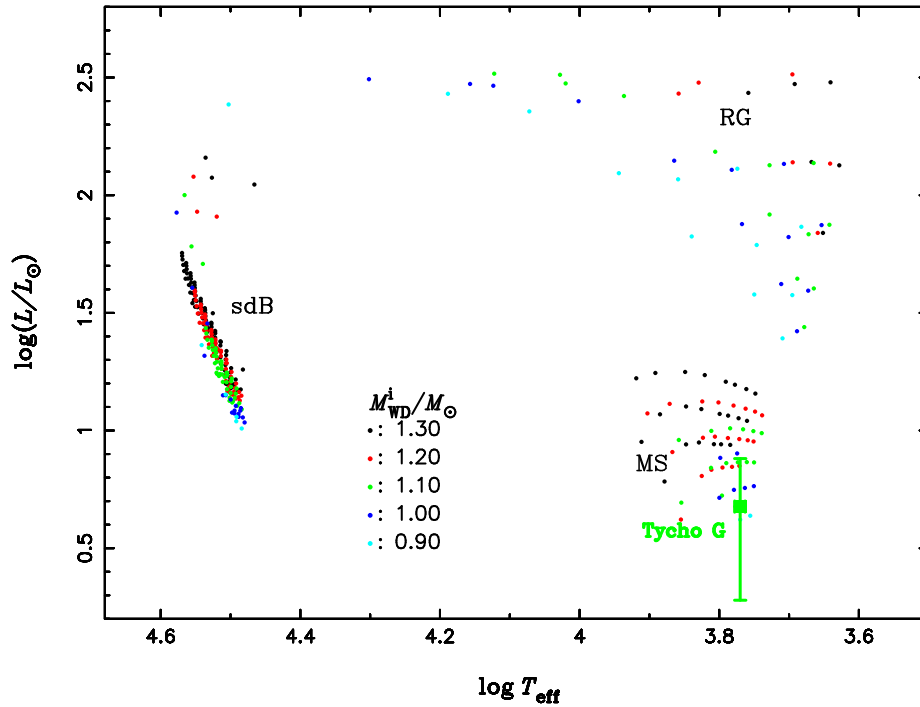


Figure 2. The evolutionary stages of the companions at the moment of supernova explosion in HR diagram, where different color points represent different initial WDs. The labels of ‘MS’, ‘RG’ and ‘sdB’ show the evolutionary states of the companions at the moment of supernova explosion. Tycho G is a possible candidate of the surviving companions for Tycho’s supernova (Ruiz-Lapuente et al. 2004).

population-synthesis (BPS) simulations as the method in Meng & Podsiadlowski (2017, 2018). Here, we assume that if a WD is less massive than $1.3 M_{\odot}$ and the system is located in the $(\log P^1, M_2^1)$ plane for a SN Ia at the onset of Roche-lobe overflow (RLOF), a SN Ia occurs. We followed the evolution of 10^7 binaries, where the primordial binary samples are generated in a Monte-Carlo way with the following input assumptions: (1) a constant star-formation rate of $5M_{\odot}/\text{yr}$, or a single starburst of $10^{11}M_{\odot}$; (2) the initial mass function (IMF) of Miller & Scalo (1979); (3) a uniform mass-ratio distribution; (4) a uniform distribution of separations in $\log a$ for binaries, where a is the orbital separation; (5) circular orbits for all binaries; (6) a CE ejection efficiency of $\alpha_{\text{CE}} = 1.0$ or $\alpha_{\text{CE}} = 3.0$, where α_{CE} denotes the fraction of the released orbital energy used to eject the CE¹ (see Meng & Podsiadlowski 2017 for further details).

To search the surviving companion in a SNR, a color-magnitude diagram (CMD) is usually used. We may get the color and absolute magnitude of the companion via interpolation in the empirical color-magnitude form in Worthey & Lee (2011), and then obtain the CMD of the companion at the moment of supernova explosion. We will compare our results with the recent surveys in the remnants of SN 1006 and Kepler’s supernova (Kerzendorf et al. 2017; Ruiz-Lapuente et al. 2018). For the remnant of SN 1006, we use the empirical color transformations in Jordi (2006) to calculate the $u - g$ color used in Kerzendorf et al. (2017). To calculate the g band apparent magnitude, we adopt a remnant’s distance of 2.2 kpc, an extinction of $A_V = 0.3$ and $A_g/A_V = 1.22$ as in Kerzendorf et al. (2017). For the remnant of Kepler’s supernova, we adopt a remnant’s distance of 5.0 kpc, an extinction of $A_V = 2.7$ and $A_R/A_V = 0.748$ as in Ruiz-Lapuente et al. (2018).

¹ Note that the CE here forms on a dynamical time-scale and will also be ejected on a dynamical time-scale, which is crucial to form some special close binaries, e.g. the close binaries with hot subdwarf stars (Han et al. 2003; Xiong et al. 2017), while the CE in the CEW model is maintained on a thermal time-scale.

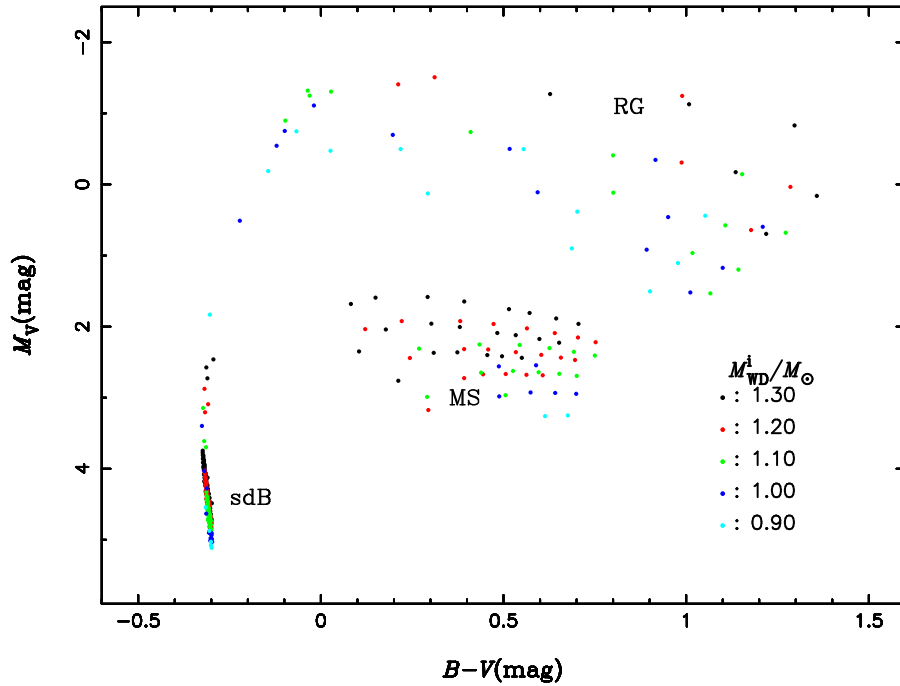


Figure 3. V band absolute magnitude, M_V , vs. $B - V$ color for the companions of SNe Ia at the moment of supernova explosion, where different color points represent different initial WDs. The labels of ‘MS’, ‘RG’ and ‘sdB’ show the evolutionary states of the companions at the moment of supernova explosion.

3 RESULT

3.1 Different evolutionary stages at the moment of supernova explosion

In Fig. 1, we show the companion evolution for three different initial binary systems, where the mass transfer between the WD and the companions begins when the companion is on the MS or in the HG. Although the initial WD mass is the same for the three systems, the final evolutionary stages of the companions at the moment of supernova explosion are quite different. For the system that the companion fills its Roche lobe on MS, the companion is still a MS star at the moment of supernova explosion for a long nuclear timescale. The other two systems have the same initial period but different initial companion mass. For the system with $M_2^i = 2.4M_\odot$, the companion is a RG star when supernova occurs, while for the system with $M_2^i = 3.0M_\odot$, the companion is a subdwarf B (sdB) star. Such different destinations are mainly derived from different mass-transfer rates between the WD and its companions. For systems with the same initial WD mass and initial orbital period, the mass-transfer rate for a system with a more massive companion is higher for a higher mass ratio, i.e. the more massive companion is more likely to lose its envelope within 10^7 yr to show the properties of a sdB star.

This result is quite different from previous concept since before this, a low mass WD was usually expected in a SNR if a spin-down timescale is considered (see the review by Nomoto & Leung 2018). The result here could potentially explain why no surviving companion was discovered in some Galactic SNRs by the most recent surveys (Kerzendorf et al. 2017; Ruiz-Lapuente et al. 2018). For the WD + He star channel, the surviving companions are also helium star, and the WD + He star channel are supported by some observations (Wang & Han 2009; McCully et al. 2014; Geier et al. 2015), but such helium stars would be much different from the sdB star predicted here. In the following subsections, we will show the properties of the companions at the moment of supernova explosion and show the differences between the sdB stars here and helium stars from the WD + He star channel.

3.2 The companions' properties at the moment of supernova explosion

3.2.1 Hertzsprung-Russell and color-magnitude diagrams

In Fig. 2, we show the evolutionary stages of the companions at the moment of supernova explosion in Hertzsprung-Russell (HR) diagram. In the figure, the companions are clearly divided into three groups, i.e. the companions may be MS, RG or sdB stars at the moment of supernova explosion². For the MS companion, the effective temperatures are between 5600 K and 8900 K and the luminosity is between $3 L_{\odot}$ and $65 L_{\odot}$, while for the RG stars, the effective temperatures are between 4000 K and 10000 K and the luminosity is between $80 L_{\odot}$ and $320 L_{\odot}$. However, the effective temperature of the sdB companions are focus around 30000 ~ 40000 K and the luminosity are between $10 L_{\odot}$ and $65 L_{\odot}$. In this paper, we do not calculate the whole model grids as in Meng & Podsiadlowski (2017), since we just focus on the SNe Ia with the sdB companions. If all the model grids are considered, some MS companions may be expected to be dimmer than $0.2 L_{\odot}$ (see the Fig. 13 in Meng & Podsiadlowski 2017)

The evolutionary state of the companions at the moment of supernova explosion heavily depends on the evolutionary state of the companion at the onset of mass transfer and the initial companion mass. In theory, for a WD + MS system, the companion fills its Roche lobe on the main sequence or in the HG, and then mass transfer begins between the WD and the companion star. If the mass transfer begins when the companion is a MS star, the companion will be still a MS star at the moment of supernova explosion for its long nuclear evolution timescale. If the mass transfer begins when the companion is crossing the HG, the final evolutionary state of the companion at the moment of supernova explosion is heavily dependent on the envelope mass upon the helium core when $M_{\text{WD}} = 1.378 M_{\odot}$. If the envelope is too thick to be consumed by mass transfer and nuclear burning within following 10^7 yr, it is a RG star at the moment of supernova. Otherwise, a sdB star is expected. Generally, for a system with given WD and companion, the longer the initial orbital period, i.e. the later the mass transfer begins, the more likely the companion to be a sdB star at the moment of supernova explosion. On the other hand, for a system with given WD and orbital period, the more massive the companion, the less massive the envelope of the companion when $M_{\text{WD}} = 1.378 M_{\odot}$ (see Figs. 7 and 9 in Meng & Podsiadlowski 2017) and then more likely the companion to be a sdB star at the moment of supernova explosion.

In Fig. 2, there is a connection between the sdB and the RG groups, i.e. the sdB stars experience a RG-like stage before they evolve to the sdB branch. In this paper, the spin-down timescale is less than 10^7 yr. It can be imagined that more companions would be at the sdB phase at the supernova explosion moment if a longer spin-down timescale is assumed.

In the figure, we also plot a possible candidate of the surviving companion, i.e. Tycho G, for Tycho's supernova. We can see that the candidate is consistent with our models with MS companions. However, for Tycho G, there are still hot arguments on whether or not it is the surviving companion of Tycho's supernova (Ruiz-Lapuente et al. 2004; Fuhrmann 2005; González Hernández et al. 2009; Kerzendorf et al. 2009; Bedin et al. 2014; Xue & Schaefer 2015).

In Fig. 3, we translate the HR diagram into the CMD with V band absolute magnitude, M_V , vs. $B - V$ color for the companions of SNe Ia at the moment of supernova explosion, which may provide potential informations for searching the surviving companion in SNRs. Again, the companions are divided into MS, RG and sdB groups and there is a connection between the RG and the sdB groups. However, the CMD presents an important information, i.e. although most of the sdB stars have a higher luminosity than the MS ones, their absolute magnitudes in V band are lower than the MS stars by 0.5 mag to 3 mag, which is derived from their high effective

² The systems with subgiant stars at the moment of supernova explosion are rare for their short lifetimes at this stage, and then we do not take the subgiant stars as a single group.

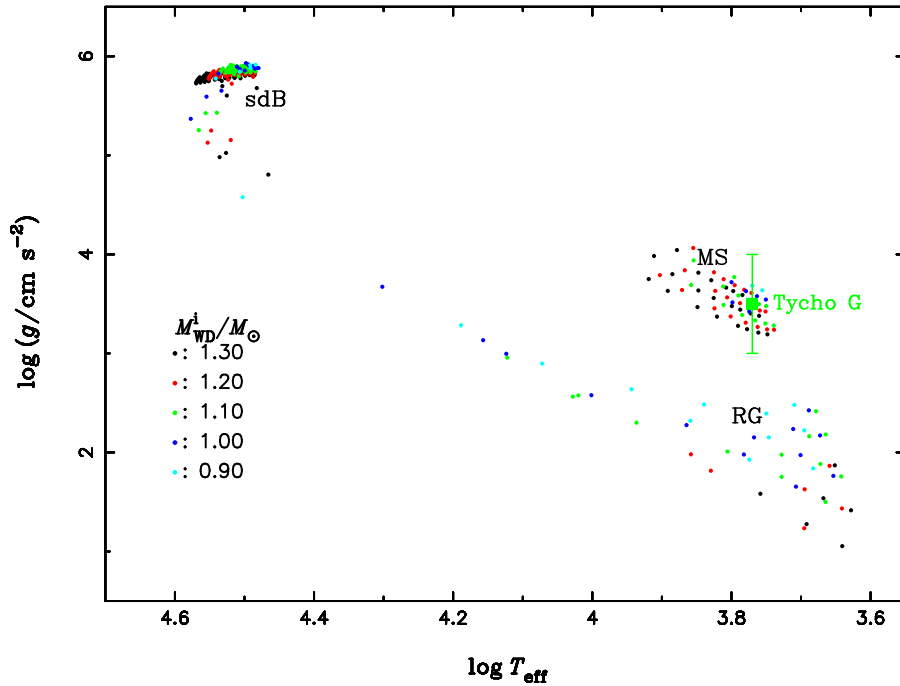


Figure 4. The gravity vs. the effective temperature of the companions at the moment of supernova explosion, where different color points represent different initial WDs. The labels of ‘MS’, ‘RG’ and ‘sdB’ show the evolutionary states of the companions at the moment of supernova explosion. Tycho G is a possible candidate of the surviving companion for Tycho’s supernova (Ruiz-Lapuente et al. 2004).

temperatures, i.e. their main radiations focus on ultraviolet band. So, U or UV band could be an ideal one to search the sdB companions.

3.2.2 Gravity

In Fig. 4, we show the gravity vs the effective temperature of the companions at the moment of supernova explosion. Again, we see the three groups and the connection between the sdB and RG groups. The three groups present their typical surface gravity, i.e. $\log g \sim 2$ for RG, ~ 3.5 for MS and ~ 6 for sdB stars.

In the figure, we also plot the possible candidate of the surviving companion, i.e. Tycho G, for Tycho’s supernova. As discussed above, its surface gravity is also consistent with the MS group predicted here.

3.2.3 Mass

To further present the properties of the companions, we show the envelope masses and the total masses of the companions at the moment of supernova explosion (Fig. 5). Here the envelope mass, M_e , is equal to the difference between the total mass and the core mass, i.e. $M_e = M_2^{\text{SN}} - M_{\text{core}}^{\text{SN}}$, where the definition of the core is the same to that in Han, Podsiadlowski & Eggleton (1994) and Meng et al. (2008). From the figure, we can see that the envelope mass of sdB companions is less than $0.03 M_\odot$, but larger than $0.01 M_\odot$, and their total masses are between $0.4 M_\odot$ and $0.65 M_\odot$, close to the typical mass of sdB stars (Heber 2009). The MS companions have a mass between $0.65 M_\odot$ and $1 M_\odot$. For RG companion, their total masses are similar to sdB stars, with an envelope of $\sim 0.1 - 0.3 M_\odot$, while the stars in the connection between the RG and the sdB stars have an envelope less massive than $0.03 M_\odot$.

After the supernova explosion, the supernova ejecta may impact into the envelope of the companions and strip off a part of the envelope (Marietta et al. 2000; Meng et al. 2007; Pakmor et al.

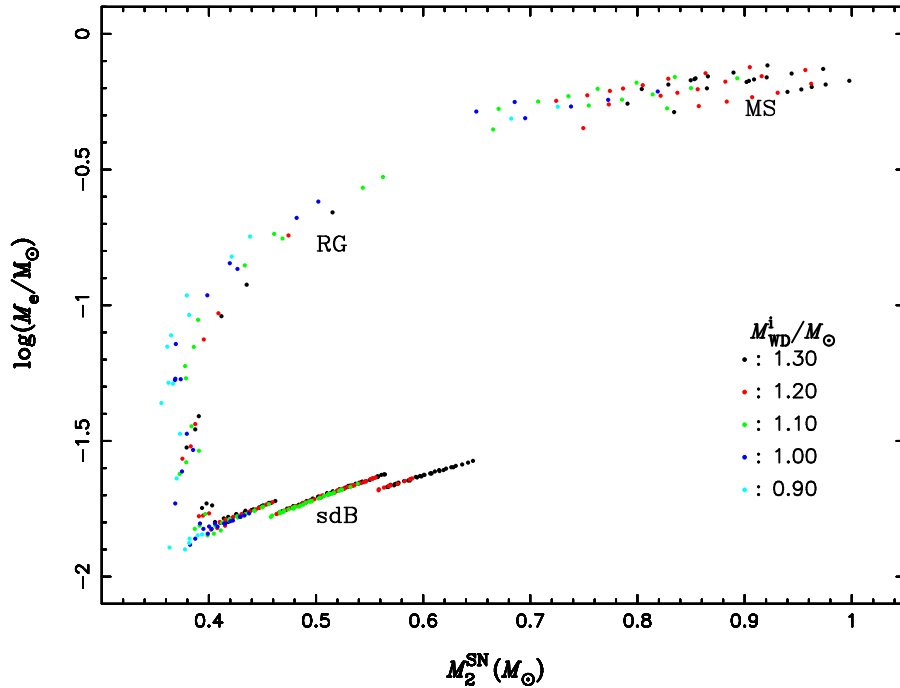


Figure 5. The envelope masses vs. the total masses of the companions at the moment of supernova explosion, where different color points represent different initial WDs. The labels of ‘MS’, ‘RG’ and ‘sdB’ show the evolutionary states of the companions at the moment of supernova explosion.

2008; Pan et al. 2012; Liu et al. 2012). So, searching the stripped-off material in the nebular spectra of SNe Ia is a method to verify the SD model. However, the deduced amount of the hydrogen-rich material from the nebular spectra of SNe Ia is usually smaller than the predicted one from numerical simulations (Mattila et al. 2005; Leonard 2007; see also Maguire et al. 2016). The negative results could be derived from the uncertainties and limitations on the radiative transfer calculation (see the discussions in Maguire et al. 2016). Another huge uncertainty is that the numerical simulations of the impact between the supernova ejecta and its companion do not consider the effect of the spin-down timescale on the companion structure. The results here are helpful to explain negative results on searching the stripped-off hydrogen-rich material in the nebular phase. For the sdB companion, there is almost no material to be stripped off, and then their total masses are almost equal to the ones presented in Fig. 5 after the impact of supernova ejecta. The MS companions are also compact than those at the time of $M_{\text{WD}} = 1.378M_{\odot}$, and then a less amount of hydrogen material are expected to be stripped off from the MS companions here (Meng et al. 2007; Pakmor et al. 2008). For the RG stars almost all the envelope will be stripped off, i.e. $\sim 0.1 - 0.3 M_{\odot}$, which is much smaller than previous value obtained by numerical simulations (Marietta et al. 2000). For the stars in the connection between RG and sdB stars, their envelopes are also very thin, and then even if the envelopes were completely stripped off, it could be difficult to detect them in the nebular spectra of SNe Ia (see also Meng & Yang 2010).

After the impact of supernova ejecta, the remnant masses of the RG companions and the ones in the connection between RG and sdB stars are close to the minimum mass for the helium ignition in the center of the star (Han et al. 2002). If the helium can be ignited in the center of the stars, they may also be sdB stars with a low mass, otherwise luminous helium WDs would be expected in SNRs (Justham et al. 2009; Meng & Yang 2010).

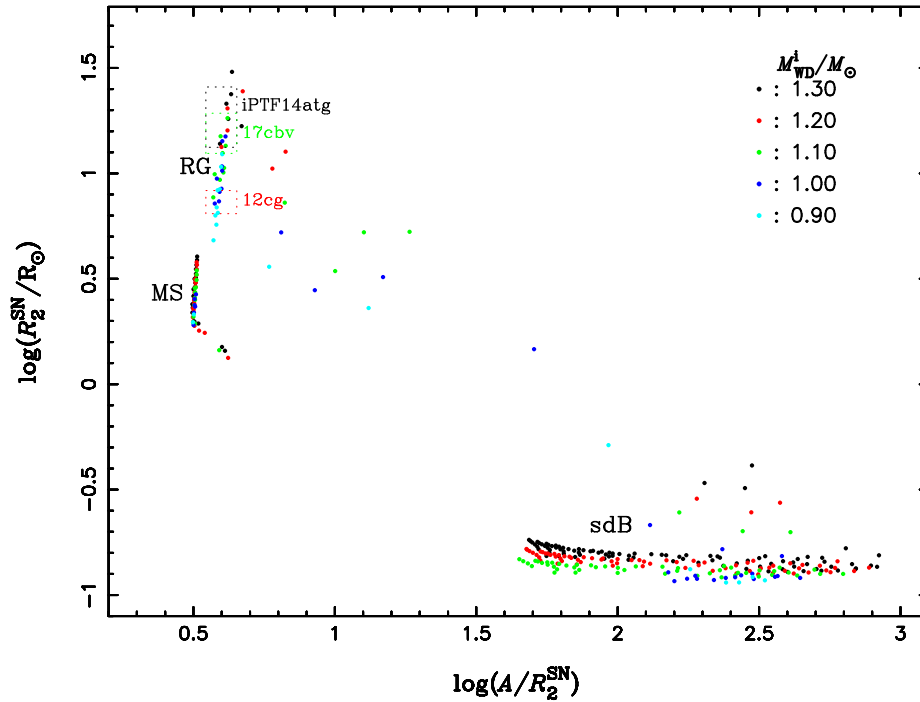


Figure 6. The companion radius and the ratio of the binary separation to the companion radius at the moment of supernova explosion, where different color points represent different initial WDs. The labels of ‘MS’, ‘RG’ and ‘sdB’ show the evolutionary states of the companions at the moment of supernova explosion. Three candidates from the SD systems, i.e. iPTF14atg, SN 2012cg and 2017cbv, are also shown by the dashed rectangles (Cao et al. 2015; Marion et al. 2016; Hosseinzadeh et al. 2017)

3.2.4 Radius and separation

The supernova ejecta collides into the companion envelope, and the kinetic energy of the supernova ejecta is transformed into the thermal energy of the envelope and finally emits in UV band (Kasen 2010). So, detecting the UV excess in the early light curve of SNe Ia is a powerful method to distinguish different progenitor models of SNe Ia (Brown et al. 2012a; Olling et al. 2015; Cao et al. 2015; Marion et al. 2016; Hosseinzadeh et al. 2017). For a Roche lobe-filling companion, the luminosity from the collision is proportional to the binary separation (Eq. 22 in Kasen 2010). Whether or not the UV excess may be detected heavily depends on the viewing angle looking down on the collision region (Kasen 2010; Brown et al. 2012a).

In Fig. 6, we show the companion radius and the ratio of the binary separation to the companion radius at the moment of supernova explosion. In the figure, the companions are divided into two sequences, i.e. the MS and RG companions follow a sequence with $\log(A/R_2^{\text{SN}}) \sim 0.6$ and the sdB stars follow the one with $\log(A/R_2^{\text{SN}})$ from 1.6 to 3. Such a difference is derived from the fact that in our model, most of the MS and RG companions are still filling their Roche lobes at the moment of supernova explosion, while the mass transfer between the WD and its companion stops for sdB companions before supernova explosion. For MS companions, there is a tail, in which the systems are detached. Similarly, the systems in the connection between the RG and the sdB groups are also detached. From the figure, we can conclude that the energies received by the sdB stars from the kinetic energy of the supernova ejecta is lower than those MS and RG companions by a factor of 10^2 to 10^5 , i.e. the UV excess from the collision between supernova ejecta and the companion can not be detected if the companion is a sdB star at the moment of supernova explosion, whatever the viewing angle is. This result is helpful to explain why so few SNe Ia show signs of UV excess among the hundreds of SNe Ia (see also the discussion in Meng & Han 2016).

In Fig. 6, we also present three candidates of SNe Ia from the SD systems, i.e. iPTF14atg, SN

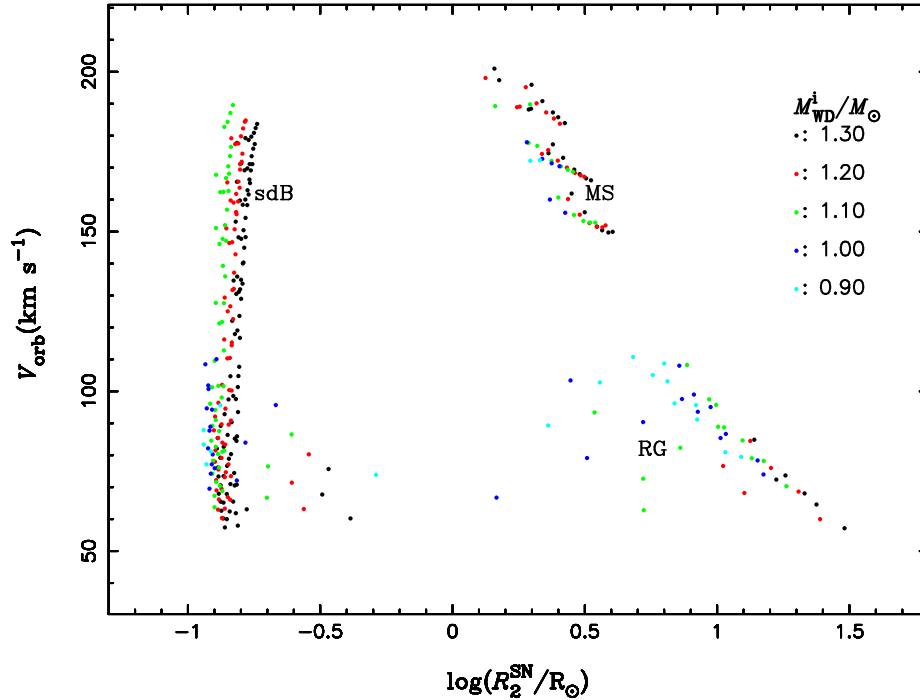


Figure 7. The companion orbital velocity relative to binary centroid vs. the companion radius at the moment of supernova explosion, where different color points represent different initial WDs. The labels of ‘MS’, ‘RG’ and ‘sdB’ show the evolutionary states of the companions at the moment of supernova explosion.

2012cg³ and 2017cbv (Cao et al. 2015; Marion et al. 2016; Graur et al. 2016; Hosseinzadeh et al. 2017). All the three SNe Ia are consistent with our RG companions. This is a natural result since the larger the separation, the higher the luminosity from the collision for a Roche lobe-filling companion (Kasen 2010). For a similar value of A/R_2^{SN} between MS and RG companion, the larger the companion radius, the higher the luminosity from the collision. As shown in Fig. 6, the MS companions have a radius between $1.2R_\odot$ and $4.5R_\odot$, while the RG companions have a radius between $6.0R_\odot$ and $32R_\odot$. So, it is more likely to detect the UV excess from the system with a RG companion than the one with a MS companion. In Marion et al. (2016), the SN 2012cg is suggested to be from a SD system with a MS star of $6M_\odot$. Actually, based on our detailed binary evolution, no any companion is as massive as $6M_\odot$ at the moment of supernova explosion (see also Meng & Podsiadlowski 2017). From Fig. 6, the progenitor of SN 2012cg is more likely to be a low-mass RG companions if the system is from a SD system (see also Boehner et al. 2017). The sdB companions usually have a radius from $0.1R_\odot$ to $0.2R_\odot$, a typical value for sdB stars (Heber 2009).

3.2.5 *Orbital and rotational velocities*

To judge the origin of a star in a SNR, its kinetics characteristics may provide very important information. Generally, except for being stripped-off a part of its envelope, the companion may receive a velocity kick from the supernova ejecta, but the kick velocity is usually much smaller than the orbital velocity (Marietta et al. 2000; Meng et al. 2007; Pakmor et al. 2008; Pan et al. 2012; Liu et al. 2012). Then, the orbital velocity of the companion at the moment of supernova explosion may represent its final space velocity to a great extent, especially for the sdB companions here, which almost do not receive any kick velocity for their large value of A/R_2^{SN} . If the spatial

³ There is still argument on whether or not SN 2012cg is from the SD system (Shappee et al. 2018).

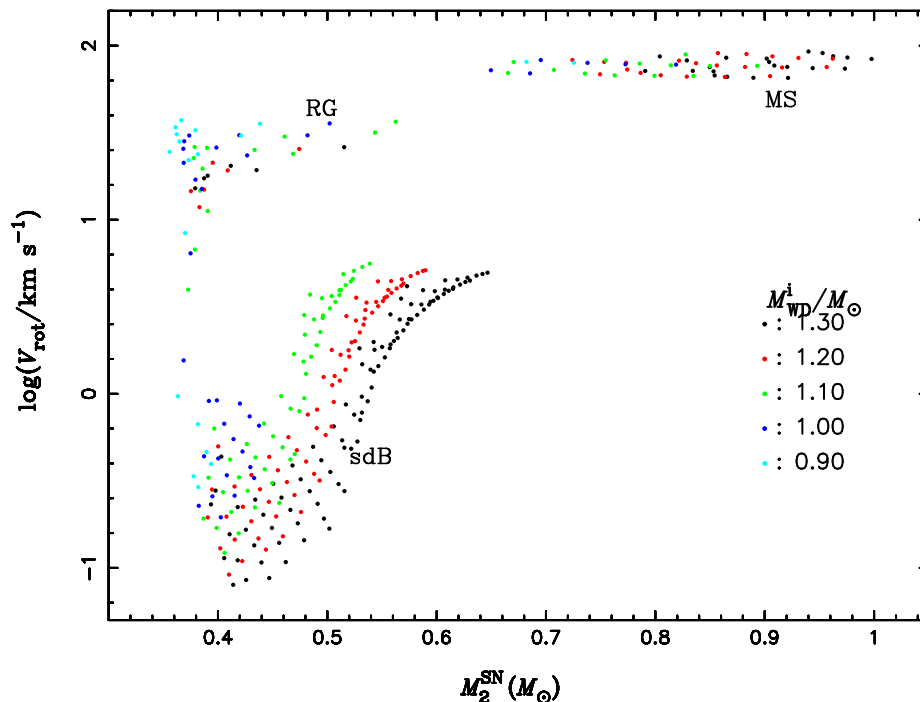


Figure 8. The equatorial rotational velocity of the companion vs. the companion mass at the moment of supernova explosion, where different color points represent different initial WDs. The labels of ‘MS’, ‘RG’ and ‘sdB’ show the evolutionary states of the companions at the moment of supernova explosion.

velocity of a star in a SNR is very different from the others in the SNR, the star is very possible to be the surviving companion in the remnant (Ruiz-Lapuente et al. 2004). In Fig. 7, we present the companion orbital velocity relative to binary centroid vs. the companion radius at the moment of supernova explosion. From the figure, we can see that different companions may have very different orbital velocity. For MS companions, the orbital velocity is from 150 km s^{-1} to 200 km s^{-1} , while the RG companions have an orbital velocity of 50 km s^{-1} to 110 km s^{-1} . For the sdB companions, the orbital velocity covers a large range, from 50 km s^{-1} to 190 km s^{-1} . Such a large range is mainly derived from the large initial orbital period range for the systems producing sdB companions, i.e. $\log(P^i/d)$ is from ~ 0.4 to 1.2 . In other words, although the mass transfer between a binary system must begin in HG for producing a sdB companion, it may occur at the stage very close to the MS end or at the end of the HG. The upper limit of the orbital velocity here is lower than that in Meng & Podsiadlowski (2017) by 60 km s^{-1} , which originates from the fact that after $M_{\text{WD}} = 1.378 M_{\odot}$, the binary orbital period increases with mass transfer for a reversed mass ratio (see Fig. 2 in Meng & Podsiadlowski 2017). For the same reason, the lower limit of the orbital velocity is also lower than that in Meng & Podsiadlowski (2017).

In Fig. 8, we show the equatorial rotational velocity of the companion at the moment of supernova explosion, where the equatorial rotation velocity is calculated by assuming that the companion star co-rotates with the orbit⁴. It is clearly shown in the figure that the MS companions have the fastest rotational velocity between 60 km s^{-1} and 100 km s^{-1} , and the RG companions have a rotational velocity of 10 to 40 km s^{-1} . For the same reason mentioned in the above paragraph, the rotational velocity of the MS companions here is much lower than that in Meng & Podsiadlowski (2017) by about 100 km s^{-1} . Especially, since the RG companions do not rotate very fast, the ro-

⁴ For a single RG star, conservation of angular momentum requires a faster rotating cores than its envelope, which could mean a fast rotating WD from the RG star (Beck et al. 2012). However, the observed sdB stars are generally slowly rotating, which could be from their much larger radii by a consideration of the conservation of angular momentum (Heber 2009, 2016).

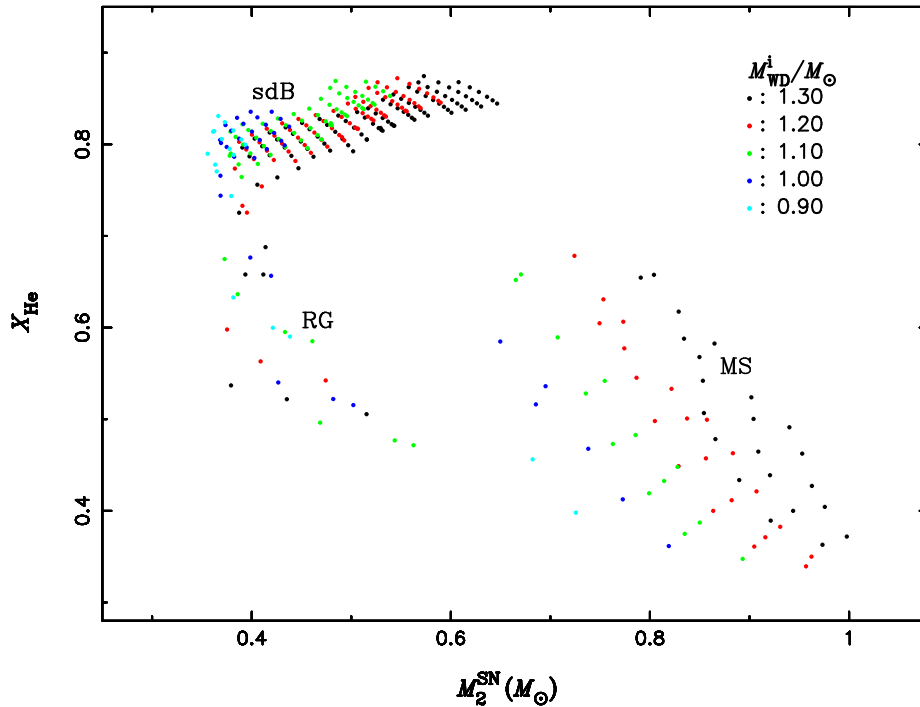


Figure 9. The surface helium abundance of the companion vs. the companion mass at the moment of supernova explosion, where different color points represent different initial WDs. The labels of ‘MS’, ‘RG’ and ‘sdB’ show the evolutionary states of the companions at the moment of supernova explosion.

tational velocity could not be a good clue to exclude a RG star as the surviving companion in a SNR. For their small radii and long orbital periods, the rotational velocity of the sdB companions is lower than 6 km s^{-1} , as low as 0.1 km s^{-1} . So, the rotational velocity can not be taken as a clue to exclude a sdB star as the surviving companion in a SNR. The rotational velocity even might not be a good clue to exclude the MS star as the surviving companion since the collision between supernova ejecta and the companion may significantly reduce the rotational velocity of the companion (Meng & Yang 2011; Pan et al. 2012; Liu et al. 2013).

3.2.6 Surface helium abundance

For the SD model, the surface hydrogen-rich material of the companion is transferred onto the WD, and then the surface material of the companion at the moment of supernova explosion may become relative hydrogen-poor. In Fig. 9, we present the surface helium abundance of the companion vs. the companion mass at the moment of supernova explosion, which may be a key clue to diagnose whether or not a star in a SNR is the surviving companion, especially for MS or RG companion. We can see from the figure that all the companions are significantly helium-enriched, no matter what the companion type is, i.e. the MS, RG and sdB companions have a surface helium abundance between 0.35 and 0.7, between 0.45 and 0.83, and between 0.75 and 0.88, respectively. Except for the mass transfer between the WD and its companion, a RG may be still expected to have a higher helium abundance than a normal MS star via the first dredge up, but its surface helium abundance can not be as high as ~ 0.8 . Therefore, if a single RG star in a SNR has a significantly higher helium abundance than other RG stars, it could be surviving companion in the SNR. Similarly, a high surface helium abundance of a single MS star in a SNR increases the possibility of the MS star as the surviving companion in the SNR. For example, the properties of an evolved MS-like star in the center region of N103B are similar to the prediction in Podsiadlowski (2003). If it is the surviving companion, it could have a high surface helium abundance. In addition, the sdB

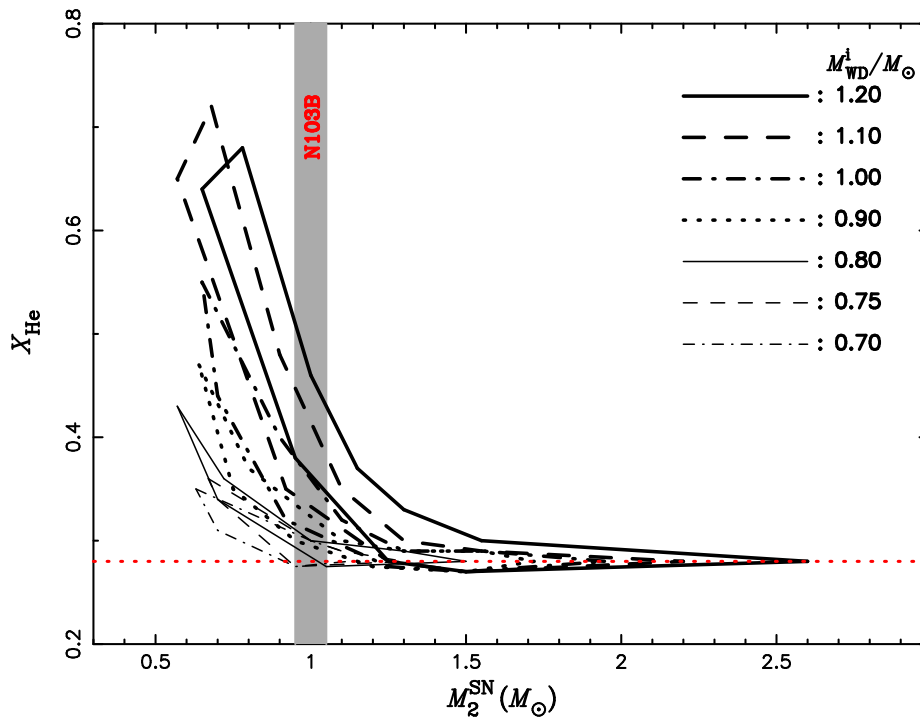


Figure 10. The contour of the surface helium abundance of the companion vs. the companion mass when $M_{\text{WD}} = 1.378M_{\odot}$ for different initial WD masses, where the data are from Meng & Podsiadlowski (2017). The dotted line shows the initial value of the helium abundance of the companions. The shaded region shows the possible value of the progenitor candidate in the SNR N103B, where the companion mass is assumed to be $1M_{\odot}$ based on the simulation in Podsiadlowski (2003).

stars here have an intermediate surface helium abundance, while those in close binaries from the canonical CE ejection channel have either a very high or a very low surface helium abundance (Xiong et al. 2017).

As a comparison, we also show the surface helium abundance of the companions when $M_{\text{WD}} = 1.378M_{\odot}$. From the figure, we can see that many systems may still produce the companions with the high surface abundance, i.e. the companions with a mass of larger than $1.5M_{\odot}$ still have an initial value of the helium abundance, while for the companions with a mass of less than $1M_{\odot}$, the helium abundance is larger than its initial value. In addition, a massive initial WD is more likely to lead to the companions with the high surface helium abundance, and then some companions with a mass of $1M_{\odot}$ to $1.5M_{\odot}$ when $M_{\text{WD}} = 1.378M_{\odot}$ also have a high surface helium abundance for the systems with the initial massive WDs. The stars with the high surface helium abundance are from those that companions fill their Roche lobe in HG, and will become the sdB or RG companions if there is a spin-down timescale. So, whatever the spin-down timescale is, there are some companions with the high surface helium abundance at the moment of supernova explosion. Therefore, if a star in a SNR has a significantly higher surface helium abundance than other stars in the SNR, the star is very likely to be the surviving companions in the SNR. In Fig. 10, we also show the possible region of the helium abundance for the candidate of the surviving companion in N103B, assuming a mass of $1M_{\odot}$ based on the simulation in Podsiadlowski (2003). It is clearly shown in the figure that the candidate would have a surface helium abundance larger than its initial value if it is the surviving companion in N103B, even though no spin-down timescale is assumed. Then, if the future spectra observation may verify that the surface helium abundance of the candidate is significantly higher than the other stars in N103B, the star is very likely to be the surviving companion.

3.2.7 *The differences from the WD + He star channel*

Here, our model predicts that if there is a delay time of a few 10^6 yr for the rapidly rotating WD to explode, the companion may be a sdB star even if the initial binary system is a WD + MS system, i.e. the surviving companion in a SNR may be a sdB star. Whatever, a sdB companion is not a new result since the surviving companion may also be a helium star for the WD + He star channel (Wang et al. 2009; McCully et al. 2014; Geier et al. 2015). However, the sdB companions predicted here are quite different from those from the WD + He star channel. In the followings, we summarize the main differences between the sdB companions here and those from the WD + He star channel.

1) There is not any hydrogen on the surviving companion from the WD + He star channel, while a thin hydrogen envelope on the sdB stars here is expected.

2) For the existence of the hydrogen envelope, the effective temperature of the companions here is much lower than that from the WD + He star channel, e.g. the effective temperature of the companions from the WD + He star channel is higher than 5×10^4 K, even higher 10^5 K (Wang & Han 2009), but it is less than 4×10^4 K here. In other words, the companions from the WD + He star channel will show the properties of extreme helium-rich subdwarf O (sdO) stars. For example, both US 708 and J2050, the suggested surviving companions of SNe Ia from the WD + He star channel, are such extreme helium-rich sdO stars (Geier et al. 2015; Ziegerer et al. 2017).

3) Before a companion star evolves to the sdB branch, the star experiences a RG-like phase (see the connection between sdB and RG groups in Fig. 2), i.e. the separation of the binary system here is much larger than that from the WD + He star channel. Especially, the system becomes a detached binary system, rather than with a Roche-lobe filling companion. Then, the orbital velocity and the rotational velocity of the companion here are much lower than those from the WD + He star channel, i.e. the orbital velocity of the sdB companion here is smaller than 190 km s^{-1} , but it is larger than 280 km s^{-1} , and its spacial velocity is higher than 350 km s^{-1} , even as high as 1200 km s^{-1} , for the helium star from the WD + He star channel (Wang & Han 2009; Geier et al. 2015).

4) Similarly, the rotational velocity of the sdB companions here is lower than 6 km s^{-1} , but it is larger than 140 km s^{-1} for the helium star from the the WD + He star channel (Wang & Han 2009).

5) The sdB companions here have a typical mass of sdB stars, i.e. from $0.4M_{\odot}$ to $0.65M_{\odot}$, while the helium star from the WD + He star channel is more massive than $0.6M_{\odot}$, even as massive as $2.0M_{\odot}$ (Wang & Han 2009). For the different masses and different evolutionary stages, the surface gravity of the sdB companions here is usually higher than that of the helium star from WD + He star, i.e. the sdB companions here have a surface gravity of $\log g \sim 6$, while the surface gravity of the helium stars from WD + He star is usually lower than 6, even as low as 4.5 (Wang & Han 2009).

6) After the supernova explosion, the supernova ejecta may inject into the companion envelope, and then the helium companion may become very luminous, e.g. the luminosity of the helium star companion may be as high as $10^4 L_{\odot}$ (Pan et al. 2014). However, the solid angle of the sdB companion to the explosion center is very small here, i.e. about $1/2000$ to $1/10^6$ of the supernova ejecta is injected into the sdB companion, and then the supernova ejecta almost can not significantly change the brightness of the sdB companions. In other words, the brightness of a sdB companion in a SNR does not significantly deviate from its brightness at the moment of supernova explosion. Even the impact of the supernova ejecta were not considered, the surviving helium star from the WD + He star channel is still much brighter than the sdB companion here, e.g. the helium star may have a luminosity of $10^2 L_{\odot}$ to $10^5 L_{\odot}$, but the luminosity of the sdB companions here is only from $10L_{\odot}$ to $65L_{\odot}$ (Wang & Han 2009; Wang et al. 2014b). Except for a lower mass,

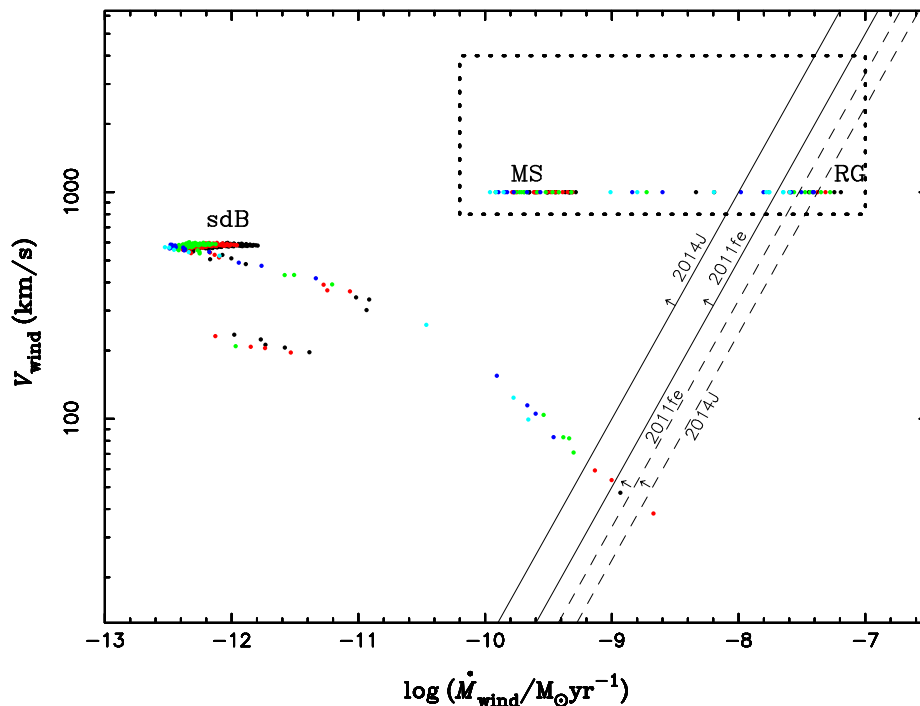


Figure 11. Wind velocity vs. mass-loss rate from the SD system at the moment of supernova explosion, where different color points represent different initial WDs. The labels of ‘MS’, ‘RG’ and ‘sdB’ show the evolutionary states of the companions at the moment of supernova explosion. The dotted rectangle shows the possible uncertainty region for wind velocity from WD surface. The left region of the solid and the dashed lines represents the permitted region for SD systems constrained by X-ray and radio observations on SN 2011fe and SN 2014J, respectively (Margutti et al. 2012, 2014; Chomiuk et al. 2012; Pérez-Torres et al. 2014).

such a luminosity difference is mainly derived from the fact that the sdB companions here are central-helium-burning, while the central helium for most of the helium star from the WD + He star channel is exhausted, i.e. they are helium RG stars (Wang & Han 2009; Wang et al. 2014b).

3.3 The mass loss rate from the binary system at the moment of supernova explosion

For a SD system, some material may lose from the binary system by wind to form circumstellar material (CSM). To search the CSM is then a key method to distinguish from different progenitor models, e.g. SN 2006X is suggested from a SD system for the discovery of the variable circumstellar Na I absorption lines in its spectra (Patat et al. 2007). If the CSM is not faraway from the explosion center, after the supernova explosion, the explosion ejecta runs into the CSM and interacts with it. If the amount of the CSM is large enough, a narrow hydrogen emission line may be observed in the spectra of the SN Ia (Hamuy et al. 2003; Silverman et al. 2013). Such SNe Ia are called as SNe Ia-CSM and are suggested to be from the hybrid CONe WD + MS systems (Meng & Podsiadlowski 2018). The emission at radio and X-ray bands is also expected from the interaction between supernova ejecta and the CSM (Chevalier 1990). Therefore, radio and X-ray observations may be wonderful tool to diagnose the progenitor origin of SNe Ia by shedding light on the properties of the CSM since CSM are generally not formed from the DD model (but see Shen et al. 2013 for a different view; Boffi & Branch 1995; Eck et al. 1995). For the two well observed SNe Ia, 2011fe and 2014J, all of the spectral, radio and X-ray observations indicate that their environments are very clear (Nugent et al. 2011; Margutti et al. 2012, 2014; Chomiuk et al. 2012; Pérez-Torres et al. 2014). In addition, no luminous object is discovered at the position of these SNe Ia in their archive images before supernova explosion (Li et al. 2011; Kelly et al. 2014). These observations seem to support that SN 2011fe and 2014J originate from the DD systems.

In Fig. 11, we show the wind velocity vs. mass-loss phase space of the binary system at the moment of supernova explosion. In the figure, we also plot the constraints from the radio and X-ray observations for SN 2011fe and 2014J (Margutti et al. 2012, 2014; Chomiuk et al. 2012; Pérez-Torres et al. 2014). In our model, for a delay timescale of a few 10^6 yr, the WDs stop increasing their masses although there is a mass transfer between the WDs and the RG companions. Mass transfer does not stop for most of the systems with the MS companions, either. However, the mass transfer stops for the sdB companions and the stars in the connection between the RG and the sdB groups. For the systems with the mass transfer, the material transferred onto the WDs is lost from the surface of the WDs, and then we assume a wind velocity of 1000 km^{-1} with an uncertainty range from 800 km^{-1} to 4000 km^{-1} (the dotted rectangle). If the mass transfer stops, the material is lost from the companion surface by a Reimers wind (Reimers 1975), where we assume a wind velocity of a half of the escape velocity of the companions.

It is clearly shown in Fig. 11 that for the systems without mass transfer, their mass loss rate is very low, even lower than $10^{-12} M_{\odot}/\text{yr}$, i.e. the environment around such SNe Ia is very clear. For those with mass transfer, the environment around SNe Ia with MS companions is also relative clear, but not as clear as those with the sdB companions. The CSM around the SNe Ia with the RG companions may be dense enough to be detected by present radio and X-ray observation. Of course, the spectral observation may also detect the CSM around the SNe Ia with RG companions. This result may explain why the SNe Ia with the CSM tend to be from the WD + RG systems (Patat et al. 2007; Dilday et al. 2012). From Fig. 11, we can see that even for the most well observed SN 2011fe and 2014J, our results still leave rather large parameter range for the SD model. Especially, if the companion stars of SN 2011fe and SN 2014J are sdB or low-mass MS stars, their clear circumstance (Nugent et al. 2011; Margutti et al. 2012, 2014; Chomiuk et al. 2012; Pérez-Torres et al. 2014) and negative results to search the stripped-off hydrogen-rich material in their nebular phase (Shappee & Stanek 2011; Shappee et al. 2013; Lundqvist et al. 2015) and negative results for searching the progenitor systems in their archive images (Li et al. 2011; Kelly et al. 2014) may be simultaneously explained. Based on the study in Meng & Han (2018), the initial WD masses of SN 2011fe and 2014J tend to be relatively small, while the progenitors producing the sdB companions usually have a massive initial WD. So, the companions of SN 2011fe and 2014J are more possible to be the low-mass MS stars if they are from the SD systems (see also Brown et al. 2012b).

In Fig. 11, there is tail for the sdB stars, which are those in the connection between the sdB and the RG groups in Fig. 2. For this systems, the mass transfer stops and the envelope of the companions is very thin (see Fig. 5). There is another small group under the sdB companions, which consists of the MS companions without filling their Roche lobe (see also the MS tail in Fig. 6)

3.4 The WD mass at the moment of supernova explosion

The WD mass at the moment of supernova explosion could play a key role on the final brightness of a SN Ia (Hachisu et al. 2012b; Wang et al. 2014a). The WD may exceeds $1.378 M_{\odot}$ if it rotates rapidly (Nomoto, Thielemann & Yokoi 1984; Yoon, Langer & Scheithauer 2004; Yoon & Langer 2005), and the mass of the WD depends on its rotational pattern. For pure rigid rotation, the WD may be as massive as $\sim 1.5 M_{\odot}$, and the the WD with a mass of larger than $1.5 M_{\odot}$ is differential rotating (Saio & Nomoto 2004; Yoon, Langer & Scheithauer 2004; Yoon & Langer 2005; Hachisu et al. 2012a). For the extreme differential rotation case, the WD may even be stable as massive as $4 M_{\odot}$ (Ostriker & Bodenheimer 1968). Here, instead of solving the detailed stellar structure of a WD, we assume the same WD growth pattern as $M_{\text{WD}} < 1.378 M_{\odot}$ as did in Wang et al. (2014a) (see also Chen & Li 2009; Hachisu et al. 2012a), and then, we may obtain the final WD

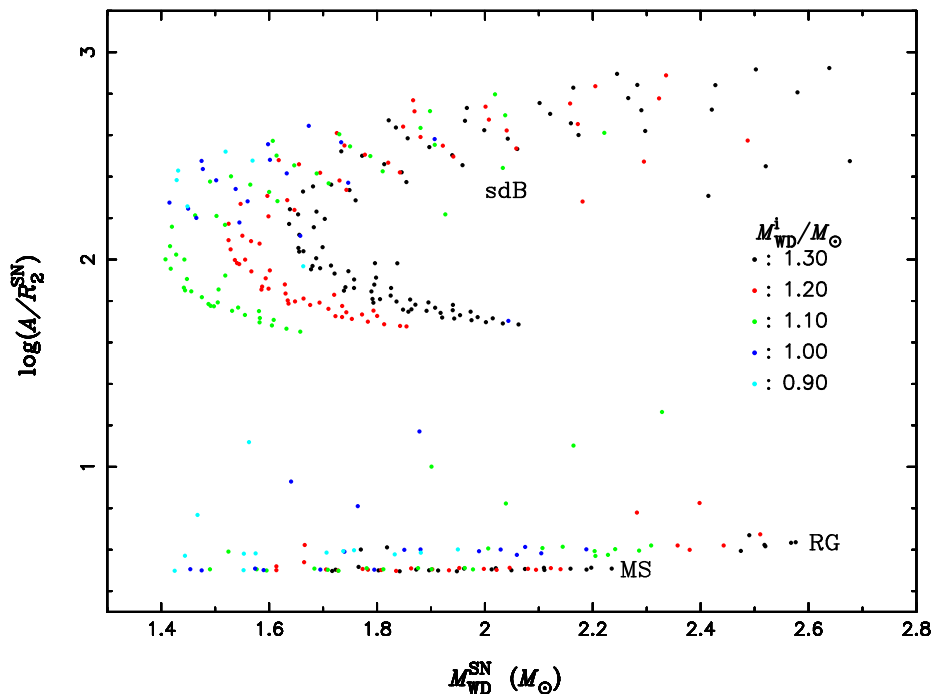


Figure 12. The ratio of binary separation to the secondary radius vs. the WD mass at the moment of supernova explosion, where different color points represent different initial WDs. The labels of ‘MS’, ‘RG’ and ‘sdB’ show the evolutionary states of the companions at the moment of supernova explosion.

mass at the moment of supernova explosion. In Fig. 12, we show the ratio of binary separation to the secondary radius vs. the WD mass. From the figure, we can see that the WD mass covers a large range, i.e. the WD mass may be as massive as $2.7 M_{\odot}$. In addition, the maximum final mass that a WD may reach is determined by its initial mass, i.e. the more massive the initial WD, the more massive the maximum final mass. However, it must be emphasized that the WD mass shown in Fig. 12 should be taken as an upper limit, which is derived from our assumption. For example, after $M_{\text{WD}} > 1.378 M_{\odot}$, the thermonuclear nuclear luminosity may exceed the Eddington luminosity of the WD for the assumption here, and then a super-Eddington wind is expected, which may reduce the timescale that the system stay in the CE phase, and then the final WD mass (see Meng & Podsiadlowski 2017).

The rapidly rotating WDs with super-Chandrasekhar mass are suggested to be the progenitor candidate of super-luminous SNe Ia (Chen & Li 2009; Hachisu et al. 2012a; Wang et al. 2014a). However, there are still many uncertainties on this subject. Firstly, it is generally accepted that the maximum brightness of a SN Ia is determined by the amount of ^{56}Ni produced during the explosion, but the final production of ^{56}Ni for the rapidly rotating WDs is heavily dependent on whether or not a detonation may be ignited in the WD (Pfannes et al. 2010a,b; Fink et al. 2018). Even a detonation is ignited, the explosion could not fit the properties of super-luminous SNe Ia, i.e. it’s difficult to reproduce the low ejecta velocity of super-luminous SNe Ia (Pfannes et al. 2010a,b; Fink et al. 2018). Secondly, as seen from the Fig. 12, a high initial WD mass is necessary to produce a significant super-Chandrasekhar mass WD (see also Wang et al. 2014a). However, a high initial mass WD may be an hybrid CONe WD, rather than a CO WD (Denissenkov 2013; Chen et al. 2014). The explosion of the hybrid CONe WDs are suggested to produce sub-luminous 2002cx-like SNe Ia, rather than super-luminous SNe Ia (Meng & Podsiadlowski 2014, 2018; Wang et al. 2014b). In addition, for some super-luminous SNe Ia, a super-Chandrasekhar mass WD could not be necessary (Scalzo et al. 2012) and even for those showing the properties of super-Chandrasekhar mass progenitor, it is more possible to be from a merger of two massive

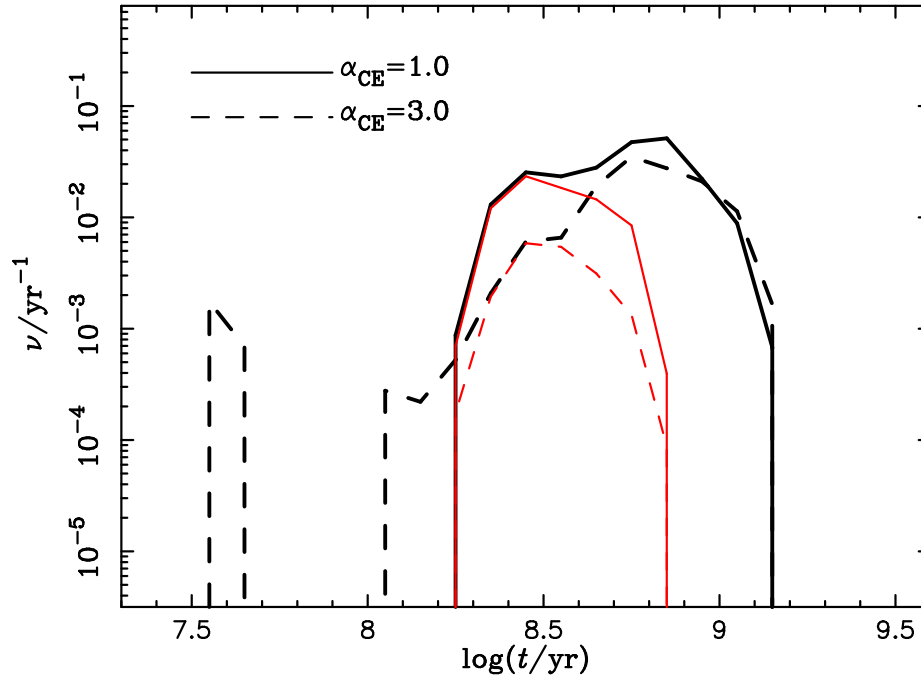


Figure 13. The evolution of the birth rates of SNe Ia for a single starburst of $10^{11} M_{\odot}$. The solid and dashed curves show the cases with $\alpha_{\text{CE}} = 1.0$ and $\alpha_{\text{CE}} = 3.0$, respectively. The black lines show the total birth rate from the WD + MS channel (Meng & Podsiadlowski 2017, 2018), while the red lines show the cases with sdB companions.

CO WDs (Taubenberger et al. 2013). As discussed above, it is still unclear which kind of SNe Ia associate with the rapidly rotating super-Chandrasekhar-mass WD predicted here.

3.5 The birth rate of SNe Ia with the sdB companions

In this paper, we suggest for the first time here that the companion of a SN Ia may be a sdB star, although its progenitor system is a WD + MS one. This is a quiet new result since a low mass WD is usually expected in a SNR if a spin-down timescale is considered (Nomoto & Leung 2018). The question is how common the sdB companions are for SNe Ia. Fig. 13 show the evolution of the birth rate of SNe Ia for a single starburst, where the black lines show the total birth rate from the WD + MS channel, while the red lines show the cases with sdB companions. Most SNe with the sdB companions occur between 160 and 800 Myr after the starburst and the birth rate peaks at ~ 300 Myr. As expected, the birth rate of SNe Ia with the sdB companions is lower, but not much lower than the total birth rate of SNe Ia. For the black dashed line, there is an alone spike at ~ 40 Myr, which is from the He star channel, as defined in Meng et al. (2009), in which primordial primary fulfills its Roche lobe in the HG or on the RG branch (see also Meng & Podsiadlowski 2014).

Fig. 14 shows the Galactic birth rates of SNe Ia from the WD + MS systems, where the red lines are for SNe Ia with the sdB companions. The birth rate of SNe Ia with the sdB companions is between $7.5 \times 10^{-5} \text{yr}^{-1}$ and $3.2 \times 10^{-4} \text{yr}^{-1}$, i.e. the SNe Ia with the sdB companions roughly contribute to 7.3% to 22% of all SNe Ia from the WD + MS channel, depending on the α_{CE} value. As discussed in section 3.2.1, if the spin-down timescale is longer than the value assumed here, the contribution of SNe Ia with the sdB companions will become higher.

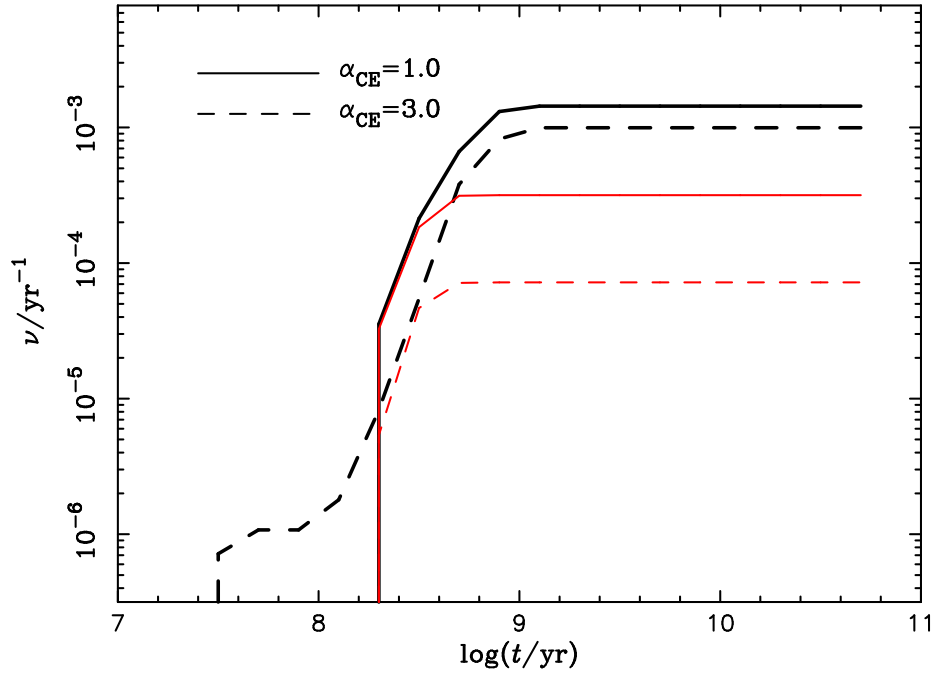


Figure 14. The evolution of the birth rates of SNe Ia for a constant SFR of $5M_{\odot}/\text{yr}$. The solid and dashed curves show the cases with $\alpha_{\text{CE}} = 1.0$ and $\alpha_{\text{CE}} = 3.0$, respectively. The black lines show the total birth rate from the WD + MS channel (Meng & Podsiadlowski 2017, 2018), while the red lines show the cases with sdB companions.

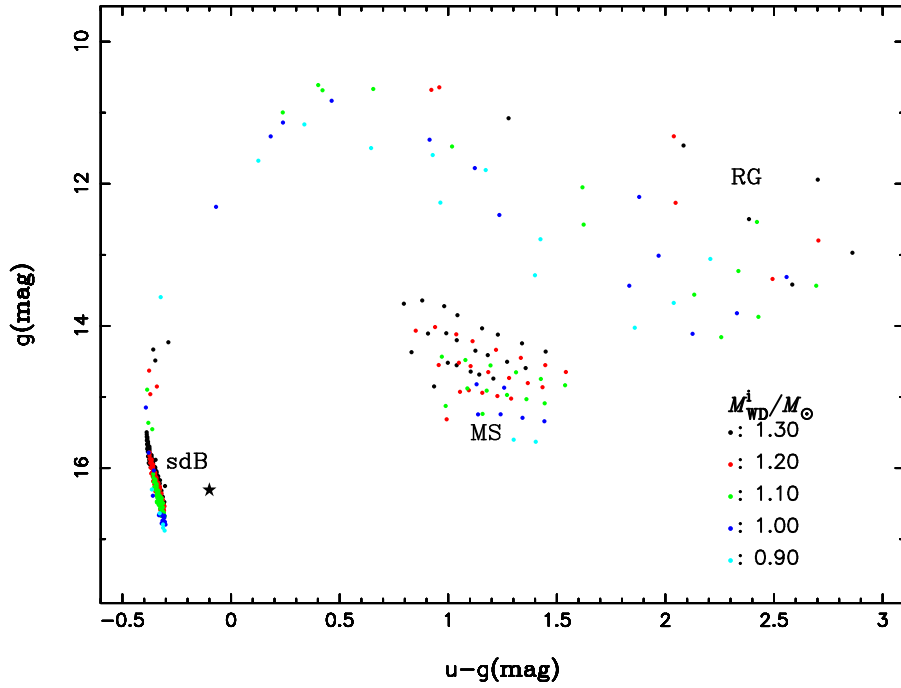


Figure 15. Similar to Fig. 3, but for g band apparent magnitude vs. $u-g$ color for the companions of SNe Ia at the moment of supernova explosion for SN 1006, where different color points represent different initial WDs. The labels of ‘MS’, ‘RG’ and ‘sdB’ show the evolutionary states of the companions at the moment of supernova explosion. The star shows a possible candidate of the surviving companion for SN 1006 (Kerzendorf et al. 2017).

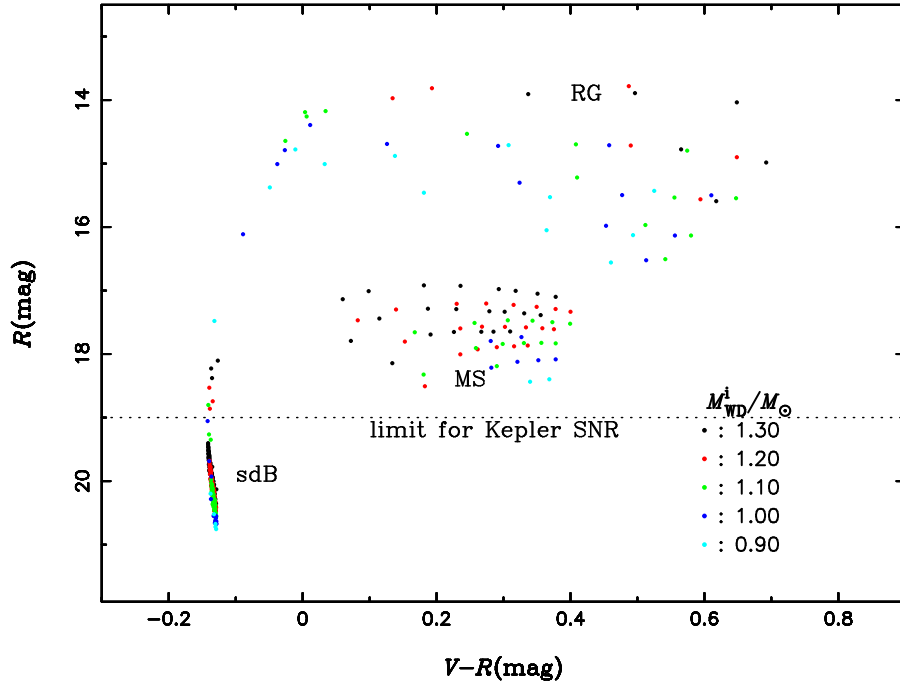


Figure 16. Similar to Fig. 3, but for R band apparent magnitude vs. $V-R$ color for the companions of SNe Ia at the moment of supernova explosion for Kepler’s supernova, where different color points represent different initial WDs. The labels of ‘MS’, ‘RG’ and ‘sdB’ show the evolutionary states of the companions at the moment of supernova explosion. The dotted line shows the limiting apparent magnitude of the R band in the survey of Ruiz-Lapuente et al. (2018).

3.6 Comparison with the survey in the remnants of SN 1006 and Kepler’s supernova

In this section, we directly compare our result with the survey results in the remnants of SN 1006 and Kepler’s supernova. The CMD of the surviving companions predicted by our model for SN 1006 is shown in Fig. 15, which is similar to Fig. 3 but for g band apparent magnitude vs. $u-g$ color. The observation in Kerzendorf et al. (2017) is deep enough to detect the surviving companion of SN 1006 if it is a MS or RG star predicted here, but neither a MS nor a RG star in the remnant was suggested to be the surviving companion (González Hernández et al. 2012; Kerzendorf et al. 2012). A sdB star could be an interesting alternative. Interestingly, a candidate in the sample of Kerzendorf et al. (2017) is quite similar to our predicted sdB stars, with a slightly redder color (the star in Fig. 15). If the candidate is the surviving companion of SN 1006, the redder color would be partly derived from reddening by dust and the collision between supernova ejecta and the companion (Podsiadlowski 2003; Pan et al. 2014, see discussions in section 4.2).

The main X-ray features of the remnant of Kepler’s supernova may be well explained by a symbiotic binary with a white dwarf and an asymptotic giant branch (AGB) star, where the interaction between the stellar wind from the AGB star and the interstellar material plays a key role to form the present shape of the remnant (Chiotellis et al. 2012). Then, the surviving companion of Kepler’s supernova would be a luminous AGB or post-AGB star, but no such candidate was discovered (Kerzendorf et al. 2014). Similarly, the X-ray image of the N103B also needs an AGB progenitor, but a MS-like star in the N103B center is suggested to be **the** surviving companion (Li et al. 2017). Actually, based on the CEW model, a WD + MS system may also explain the X-ray features of the remnants, in which the CEW replaces the stellar wind of the AGB star. Especially, the CEW model may explain the X-ray image of the N103B and MS-like surviving companion, simultaneously.

The survey in the remnant of Kepler’s supernova by Ruiz-Lapuente et al. (2018) has a limiting apparent magnitude $m_R = +19$ mag, and the photometry and proper motions are complete down

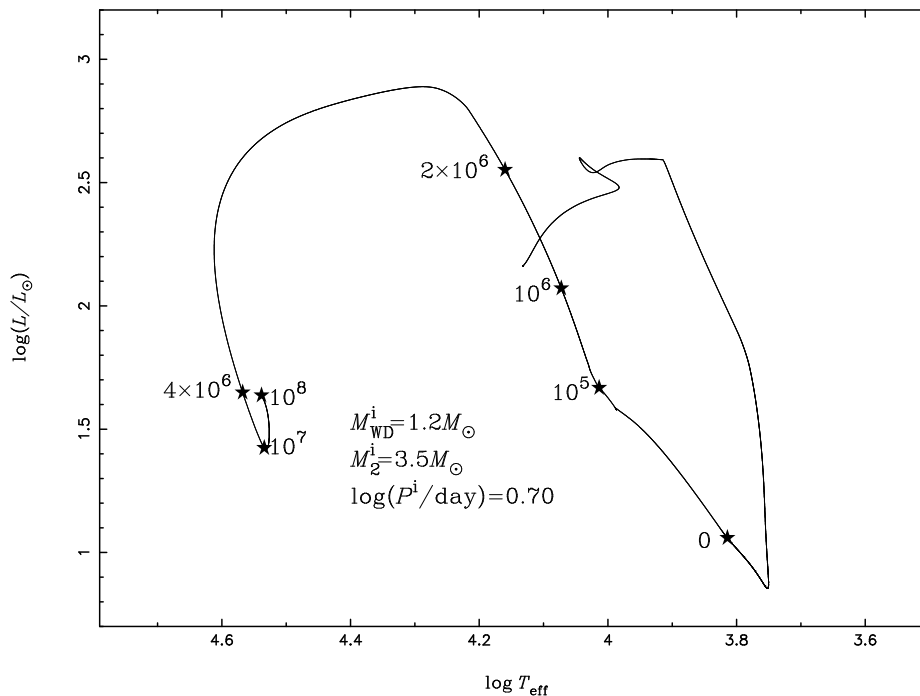


Figure 17. The evolution of the companion for the initial binary system of $[M_{\text{WD}}^i/M_{\odot}, M_2^i/M_{\odot}, \log(P^i/\text{d})] = (1.2, 3.5, 0.7)$ with different spin-down timescales.

to $m_{\text{F814W}} \simeq 22.5$, where F814W band is similar to a wide I band. In Fig. 16, we show the R band apparent magnitude vs. $V - R$ color for the surviving companions assuming a distance to Kepler’s supernova and a visual extinction in the direction to the remnant of Kepler’s supernova. Again, the figure clearly shows that the survey of Ruiz-Lapuente et al. (2018) would detect the surviving companion of Kepler’s supernova if it is a MS or a RG star. No MS or RG star is suitable to be the surviving companion of Kepler’s supernova (Ruiz-Lapuente et al. 2018). However, the survey focuses on the red bands and cannot exclude the sdB stars as the surviving companion of Kepler’s supernova, e.g. almost all the sdB stars in Fig. 16 are dimmer than the detection limit of R band in Ruiz-Lapuente et al. (2018). If a sdB star is the surviving companion of Kepler’s supernova, our model may simultaneously explain the X-ray features of the remnant and the negative reports on searching the surviving companion in the remnant. If someone wants to check whether or not a sdB star is the surviving companion of Kepler’s supernova, the survey must be as deep as $m_{\text{R}} \sim +21$ mag. Obviously, both R and F814W bands have a too long wavelength and is not a good choice to search the sdB star in the remnant of Kepler’s supernova, while U or UV band would be an excellent alternative. Whatever, a low-mass MS surviving companion is still possible for the Kepler’s supernova since the low-mass MS companion may be as dim as $0.2 L_{\odot}$ (Meng & Podsiadlowski 2017), which is much lower than the detection limit in Ruiz-Lapuente et al. (2018) by one order of magnitude.

4 DISCUSSIONS AND CONCLUSIONS

4.1 The effect of spin-down timescale on the results

In this paper, we assume a spin-down timescale of less than 10^7 yr, consistent with the empirical constraints (Meng & Podsiadlowski 2013, 2018), but the exact value of the spin-down timescale is very uncertain. Based on the simple consideration of the conservation of angular momentum, Meng & Han (2018) found that the more massive the initial WD, the shorter the spin-down

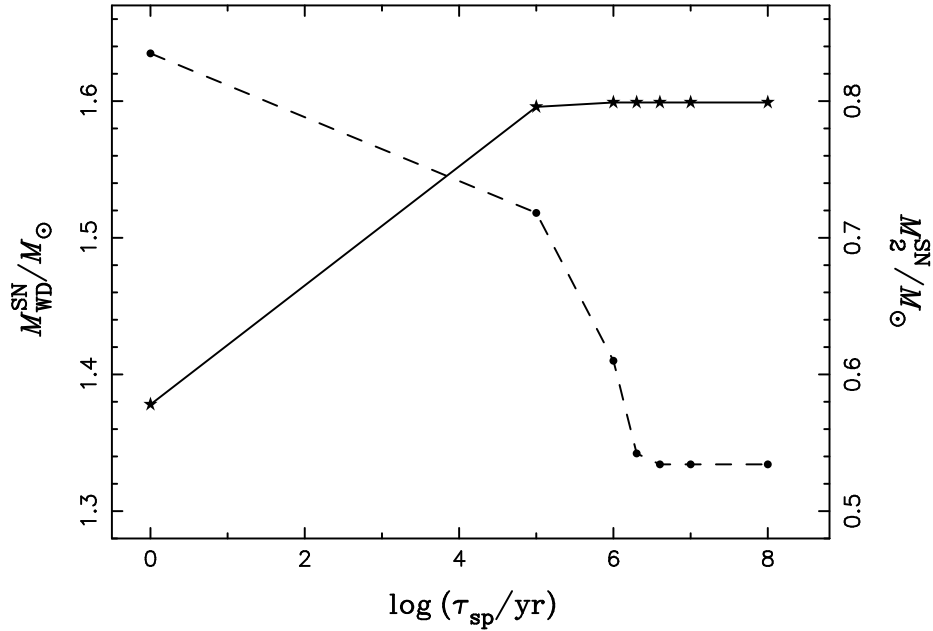


Figure 18. The final WD and companion mass for the initial binary system of $[M_{\text{WD}}^i/M_{\odot}, M_2^i/M_{\odot}, \log(P^i/d)]=(1.2, 3.5, 0.7)$ as a function of the spin-down timescale.

timescale. Here, the uncertainty of the spin-down timescale has a great impact on whether the sdB companion may be produced and on how common the SNe Ia with the sdB companions are. Here, we choose a model with the initial parameters of $[M_{\text{WD}}^i/M_{\odot}, M_2^i/M_{\odot}, \log(P^i/d)]=(1.2, 3.5, 0.7)$ to check the effect of the spin-down timescale, where the definition of the spin-down timescale here is the same to that in section 2. Fig. 17 shows the effect of the spin-down timescale on the evolution of the companion. From the figure, we can see that if the spin-down timescale is longer than $3 - 4 \times 10^6$ yr, the companion will show the properties of a sdB star at the moment of supernova explosion. Fig. 18 shows the final WD and companion masses as a function of spin-down timescale. We can see from the figure that the final WD mass does not change with the spin-down timescale if the spin-down timescale is longer than 10^6 yr, while the companion mass does not change with the spin-down timescale until the spin-down timescale is longer than $3 - 4 \times 10^6$ yr, i.e. although the WD stop increasing its mass, the companion are still losing its material by mass transfer or stellar wind. Considering that there is an uncertainty of $\sim 10^6$ yr on the onset of the spin-down phase, the discussion above means that if the real spin-down timescale is longer than $2 - 3 \times 10^6$ yr, our results are not significantly affected by the spin-down timescale. Via an empirical method, Meng & Podsiadlowski (2013) have shown that the spin-down timescale is shorter than a few 10^7 yr, and a spin-down timescale of $2 - 3 \times 10^6$ yr is consistent with the constraint in Meng & Podsiadlowski (2013).

4.2 The surviving companion in the remnant of SN 1006

Searching the surviving companions in SNRs is a powerful way to distinguish different models. At present, MS, RG and luminous WD are excluded as the surviving companion of SN 1006 (González Hernández et al. 2012; Kerzendorf et al. 2012, 2017), but sdB stars are not. Interestingly, there is indeed a star similar to our prediction in the remnant of SN 1006, although it is redder than our prediction. The star is indeed a single sdB star, i.e. the Schweizer-Middleditch (SM) star, whose distance is also consistent with the remnant of SN 1006 (Schweizer & Middleditch 1980; Winkler et al. 2003). Three main effects could contribute to the redder color of the candidate. 1)

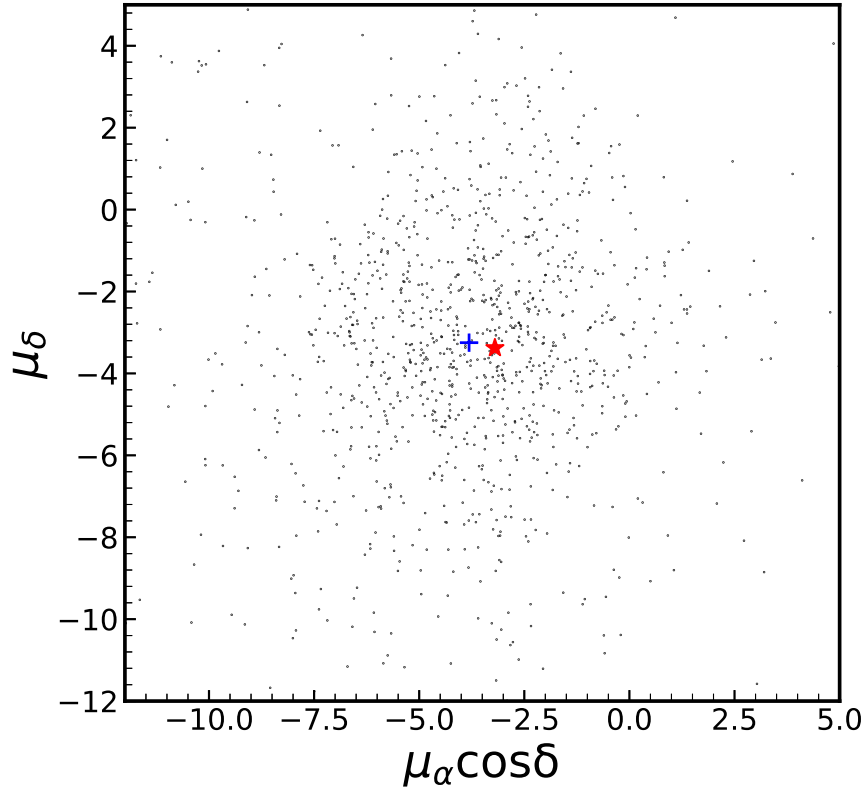


Figure 19. The proper motions of the stars within $5'$ of the remnant center of SN 1006. The blue cross presents the median value of the proper motions of the stars, while the red star represent the SM stars (Schweizer & Middleditch 1980).

Before supernova explosion, the system experiences a common envelope wind phase. With the expansion and cooling of the CE material, dust may form around the progenitor system as observed in some normal and special SNe Ia (Lü et al. 2013; Fox & Filippenko 2013; Silverman et al. 2013; Johansson et al. 2013; Fox et al. 2016). The dust could redden the color of the candidate. 2) In this paper, we do not consider the interaction between supernova ejecta and the companion. The supernova ejecta may collide into the companion and inject some kinetic energy of the supernova ejecta into the envelope, and then huff the envelope (Marietta et al. 2000; Meng et al. 2007). After the interaction, the envelope will re-establish dynamical equilibrium soon, but still in a process into thermal equilibrium, lasting for $10^3 - 10^4$ yr. During this phase, the effective temperature of the companion could be lower than that predicted here by 1000 to 3000 K depending on the ejection energy, i.e. a slightly redder color (Podsiadlowski 2003; Pan et al. 2014). However, the effect could be very small for the small solid angle of the sdB companions relative to the explosion center. 3) The dust may also form from the supernova ejecta itself and such dust may also contributes to a part of color excess (Williams et al. 2014; Rho et al. 2018). So, a redder color is not unimaginable for the SM star. Actually, the color excess of the SM star may be as large as $E(B - V) = 0.16 \pm 0.02$ (Burleigh et al. 2000). If such a color excess is considered, the color of the SM star is consistent with our prediction. In addition, the surface gravity and effective temperature of the MS star are $\log g = 6.18 \pm 0.3$ and 32900 ± 340 K, respectively, which are also consistent with our results (see Fig. 4, Burleigh et al. 2000). Moreover, there is a thin hydrogen envelope for the SM star as we predicted (Burleigh et al. 2000). Then, if the SM star is the surviving companion of SN 1006, it

must not be from the WD + He star channel, since no hydrogen on the helium companion is leaved for the WD + He star channel.

However, due to the presence of red-shifted absorption lines from SN ejecta, the SM star was suggested to be a background star, and its distance was suggested to be only slightly greater than the remnant of SN 1006 (Wu et al. 1983; Winkler et al. 2003, 2005). However, the red-shifted absorption lines could also be derived from an asymmetrical explosion as indicated by the strongly asymmetric profiles of Fe_{II} and Si_{II} line and the asymmetric distribution of the elements in the remnant (Winkler et al. 2005, 2011; Hamilton et al. 2007; Uchida et al. 2013; Zhou & Vink 2018). The asymmetric explosion could be a common properties of SNe Ia (Maeda et al. 2010).

Therefore, the kinetics characteristics of the star could be the only piece to judge whether or not the SM star is the surviving companion of SN 1006. If its space velocity is significantly different from the other stars in the remnant of SN 1006, the probability to be the surviving companion would become high. Otherwise, the probability becomes low. We check the proper motion of the stars within 5' of the remnant center from GAIA DR2, as shown in Fig. 19. From the figure, it seems that there is not difference between the SM star and other stars in the remnant of SN 1006 in the aspect of proper motion, i.e. the proper motion of the SM star only slightly deviates from the median value of the proper motions of the stars at the direction of the SNR center of SN 1006, and such a proper motion disfavors the SM star as the surviving companion of SN 1006 (Schweizer & Middleditch 1980; Burleigh et al. 2000). So, a 3D space velocity is helpful to judge the nature of the SM star. However, unfortunately, some data of the SM star in GAIA DR2 are so uncertain that we cannot use them to constrain its 3D space velocity, otherwise we could obtain a complete wrong conclusion⁵. For example, the parallax of the SM star is $\varpi = 0.0736 \pm 0.1244$, and then $\sigma_{\varpi}/\varpi = 1.69$ which is much larger than the threshold value of 0.2 for distance estimation from GAIA DR2 data (Astraatmadja & Bailer-Jones 2016; Katz et al. 2018). The distance of the SM star from this parallax is much larger than all the previous measurements from spectrum by at least a factor of 2 (see summary in Burleigh et al. 2000). Considering that some other astrometric measurements of the SM star are also very uncertain, we applied the measurements in the previous literatures as the distance of the SM star. Based on a radial velocity of $-13 \pm 17 \text{ km}^{-1}$ and a distance of $2.07 \pm 0.18 \text{ kpc}$ (Schweizer & Middleditch 1980; Winkler et al. 2003; Kerzendorf et al. 2017), we can calculate the UVW velocities of the SM star, i. e. $U = -5.2 \pm 14 \text{ km}^{-1}$, $V = 197 \pm 10 \text{ km}^{-1}$ and $W = 3.1 \pm 5 \text{ km}^{-1}$. The V value of the SM star is smaller than that of a normal disk star. We then transform these velocities into the Galactic rotational velocity at a Galactocentric distance of $\sim 6.67 \text{ kpc}$, i.e. $V_c = 196 \pm 12 \text{ km}^{-1}$, which is smaller than the Galactic rotational velocity of the disk stars at the Galactocentric distance by $50 \pm 19 \text{ km}^{-1}$ (Huang et al. 2016). This velocity difference is marginally consistent with the predicted orbital velocity here (see Fig. 7). In addition, the smaller rotational velocity of the SM star may explain its small proper motion shown in Fig. 19. So, the SM star is still possible to be the surviving companion of SN 1006.

Since we still can not completely exclude the SM star as the surviving companion of SN 1006, we propose a further detailed study on the SM star in the remnant of SN 1006. If the candidate is the surviving companion of SN 1006, it will be a great step for the progenitor study of SNe Ia. On the contrary, if it is not, e.g. the future precise distance measurement makes sure that the SM star is a background star, the survey in the remnant of SN 1006 would favor the DD model or a long spin-down timescale as suggested in Kerzendorf et al. (2017), or a hybrid explosion between core-collapse SN and SNe Ia without the surviving companion predicted in Meng & Podsiadlowski (2018).

⁵ For example, the effective temperature of the SM star in GAIA DR2 is definitely not the effective temperature of a sdB star, i.e. $8869^{+724}_{-906} \text{ K}$, which is derived from a wrong effective temperature pattern for the stars with the effective temperature of larger than 10000 K (Andrae et al. 2018).

4.3 The surviving companion in the remnant of Kepler's supernova

Similarly, no MS or RG star in the remnant of Kepler's supernova is suitable to be the surviving companion of Kepler's supernova (Ruiz-Lapuente et al. 2018). We propose a deeper survey in the remnant by a blue band to check whether there is a hot subdwarf star as we predicted. If there is, it will support the CEW model and then the SD model. Otherwise, the core-degenerate scenario would be an alternative, i.e. the Kepler's supernova could originate from the merger of a CO WD and a massive CO core of an AGB star (Kashi & Soker 2011; Ruiz-Lapuente et al. 2018), or the merger of a hybrid CONe WD with a Chandrasekhar mass and its MS companion is another alternative (Meng & Podsiadlowski 2018). Moreover, a low-mass MS star with a luminosity as dim as $0.2 L_{\odot}$ can also not be completely excluded by the observation in Ruiz-Lapuente et al. (2018).

Whatever, an question should be noticed, i.e. why do the surviving companions in the both Galactic SNRs tend to be sdB stars? Based on BPS studies here, as much as 22% of SNe Ia will explode with the sdB companions. Actually, to be a sdB star at the moment of supernova explosion, the mass transfer between the WD and its companion must begin when the companion is crossing the HG. Some binary population synthesis studies have shown that most of the binary systems indeed begin their mass transfer at the HG (e.g. see Fig. 11 in Meng et al. 2009), which means that rather a part of the surviving companions in SNRs could be the sdB stars. The CEW model even increases the probability that a sdB star is the surviving companion in a SNR. Compared with the OTW model, the parameter space leading to SNe Ia from our CEW model extends to more massive companions and to longer initial orbital period (see Fig. 7 in Meng & Podsiadlowski 2017). For the systems in the increased parameter space, the companions just tend to appear as the sdB stars at the moment of supernova explosion for a spin-down timescale assumed here. As shown in Fig. 2, there is a connection between the sdB and the RG companions, i.e. if the spin-down timescale is longer than the timescale assumed here, more companion will show the properties of the sdB stars. This could explain the negative results for searching the surviving companion in most of SNRs, since the surveys usually focus on luminous MS or RG candidate.

Since a sdB star has a life much longer than a SNR, we would expect that there are many sdB stars from SNe Ia wandering in the Galaxy. In the future, we will give a detailed study on such sdB stars from our SN Ia progenitor model.

In summary, based on the CEW model in Meng & Podsiadlowski (2017), we study the properties of the companions at the moment of supernova explosion in details, where we assume a spin-down timescale of less than 10^7 yr. We found that the companions may be the MS, RG and sdB stars, although the initial systems are WD + MS ones. Our results may explain the observations constraining the progenitors of some SNe Ia. Here, we suggest for the first time that the sdB stars as the surviving companions of SNe Ia may be from the WD + MS system. Especially, the sdB companions here are quite different from the helium companions from the WD + He star channel. The SNe Ia with the sdB companions may contribute as much as 22% to all SNe Ia. We propose a deep search for the surviving companions in some supernova remnants in U or UV bands.

ACKNOWLEDGMENTS

This work was partly supported by the NSFC (No. 11473063, 11522327, 11390374, 11521303 and 11733008), Yunnan Foundation (No. 2015HB096, 2017HC018), CAS light of West China Program and CAS (No. KJZD-EW-M06-01).

REFERENCES

- Andrae, R., Fouesneau, M., Creevey, O., et al., 2018, *A&A*, 616, A8
- Astraatmadja, T.L., Bailer-Jones, C.A.L., 2016, *ApJ*, 833, 119
- Benvenuto, O.G., Panei, J.A., Nomoto, K., Kitamura, H., Hachisu, I. 2015, *ApJ*, 809, L6
- Bedin L. R., Ruiz-Lapuente P., González Hernández, J. I., Canal R., Filippenko A. V., Mendez J., 2014, *MNRAS*, 439, 354
- Beck, P.G., Montalbán, J., Kallinger, T., et al., 2012, *Nature*, 481, 55
- Boffi, F. R., & Branch, D. 1995, *PASP*, 107, 347
- Boehner, P., Plewa, T., Langer, N., 2017, *MNRAS*, 465, 2060
- Brown, P. J., Dawson, K. S., Harris, D. W., et al. 2012a, *ApJ*, 749, 18
- Brown, P. J., Dawson, K. S., de Pasquale, M., et al. 2012b, *ApJ*, 753, 22
- Burleigh, M. R., Heber, U., O'Donoghue, D., Barstow, M. A., 2000, *A&A*, 356, 585
- Cao, Y. Kulkarni, S. R., Howell, D. A. et al., 2015, *Nature*, 521, 328
- Chen, M. C., Herwig, F., Denissenkov, P. A. & Paxton, B. 2014, *MNRAS*, 440, 1274
- Chen, W., Li X., 2009, *ApJ*, 702, 686
- Chevalier, R. A. 1990, in *Supernovae*, ed. A. G. Petschek (New York: Springer-Verlag), 91
- Chiotellis, A., Schure, K. M., & Vink, J. 2012, *A&A*, 537, A139
- Chomiuk, L., Soderberg, A., Moe, M., et al. 2012, *ApJ*, 750, 164
- Denissenkov, P. A., Herwig, F., Truran, J. W., & Paxton, B. 2013, *ApJ*, 772, 37
- Dilday B., Howell D.A., Cenko S.B. et al., 2012, *Science*, 337, 942
- Di Stefano R., Voss R., & Claeys J.S.W., 2011, *ApJL*, 738, L1
- Di Stefano R., & Kilic M. 2012, *ApJ*, 759, 56
- Eck, C. R., Cowan, J. J., Roberts, D. A., et al. 1995, *ApJ*, 451, L53
- Fink, M., Kromer, M., Hillebrandt, W., et al., 2018, *A&A*, in presee, arXiv; 1807.10199
- Fox, O.D. & Filippenko, A. V., 2013, *ApJL*, 772, L6
- Fox, O.D., Johansson, J., Kasliwal, M., et al., 2016, *ApJL*, 816, L13
- Fuhrmann K., 2005, *MNRAS*, 359, L35
- Geier, S, Fürst, F., Ziegerer, E., et al. 2015, *Science* 347, 1126
- González Hernández, J. I., Ruiz-lapuente P., Filippenko A., Foley R. J., Gal- Yam A., Simon J. D., 2009, *ApJ*, 691, 1
- González Hernández, J. I., Ruiz-Lapuente, P., Tabernero, H. M. et al., 2012, *Nature*, 489, 533
- Graur, O., Zurek, D., Shara, M. M. et al., 2016, *ApJ*, 819, 31
- Hachisu, I., Kato, M., Nomoto, K., *ApJ*, 1996, 470, L97
- Hachisu, I., Kato, M., Saio, H., Nomoto, K., 2012a, *ApJ*, 744, 69
- Hachisu, I., Kato, M., Nomoto, K., 2012b, *ApJL*, 756, L4
- Hamuy, M., Phillips, M. M., Suntzeff, N. B. et al., 2003, *Nature*, 424, 651
- Hamilton, A. J. S., Fesen, R. A., & Blair, W. P. 2007, *MNRAS*, 381, 771
- Han Z., Podsiadlowski P., Eggleton P.P., 1994, *MNRAS*, 270, 121
- Han, Z., Podsiadlowski, Ph., Maxted, P. F. L., Marsh, T. R., Ivanova, N., 2002, *MNRAS*, 336, 449
- Han, Z., Podsiadlowski, Ph., Maxted, P. F. L., Marsh, T. R., 2003, *MNRAS*, 341, 669
- Heber, U., 2009, *ARA&A*, 2009, 47, 211
- Heber, U., 2016, *PASP*, 128, 082001
- Hillebrandt, W., Niemeyer, J.C., 2000, *ARA&A*, 38, 191
- Hosseinzadeh, G., Sand, D. J., Valenti, S., et al. 2017, *ApJL*, 845, L11
- Huang, Y., Liu, X.W., Yuan, H.B., et al., 2016, *MNRAS*, 463, 2623
- Iben, I., Tutukov, A.V., 1984, *ApJS*, 54, 335
- Johansson, J., Amanullah, R., Goobar, A., 2013, *MNRAS*, 431, L43

- Jordi, K., Grebel, E. K., Ammon, K., 2006, *A&A*, 460, 339
- Justham, S., Wolf, C., Podsiadlowski, P., & Han, Z. 2009, *A&A*, 493, 1081
- Justham S., 2011, *ApJL*, 730, L34
- Kasen, D. 2010, *ApJ*, 708, 1025
- Kashi, A. & Soker, N., 2011, *MNRAS*, 417, 1466
- Katz, D., Antoja, T., Romero-Gómez, M., et al., 2018, *A&A*, 616, A11
- Kelly, P.L., Fox, O.D., Filippenko, A.V., et al., 2014, *ApJ*, 790, 3
- Kerzendorf W. E. et al., 2009, *ApJ*, 701, 1665
- Kerzendorf, W.E., Schmidt, B.P., Laird, J.B., Podsiadlowski, Ph., Bessell, M.S., 2012, *ApJ*, 759, 7
- Kerzendorf, W. E., Childress, M., Scharwächter, J., Do, T., Schmidt, B. P., 2014, *ApJ*, 782, 27
- Kerzendorf, W.E., Strampelli, G., Shen, K. J. et al. 2017, arXiv: 1709.06566
- Leibundgut, B., 2000, *A&ARv*, 10, 179
- Leonard D.C., 2007, *ApJ*, 670, 1275
- Li, C., Chu, Y., Gruendl, R. A. et al., 2017, *ApJ*, 836, 85
- Li, W.-D., Bloom, J. S., Podsiadlowski, Ph. et al., 2011, *Nature*, 480, 348
- Liu, Z. W., Pakmor, R., Röpke, F. K., et al., 2012, *A&A*, 548, A2
- Liu Z.W., Pakmor R., Röpke F.K. et al., 2013, *A&A*, 554, A109
- Lü, G., Zhu, C., Podsiadlowski, Ph., 2013, *ApJ*, 768, 193
- Lundqvist P. et al., 2015, *A&A*, 577, A39
- Maeda, K., Benetti, S., Stritzinger, M., et al. 2010, *Nature*, 466, 82
- Maoz D., Mannucci F., Nelemans G., 2014, *ARA&A*, 52, 107
- Marietta E., Burrows A., Fryxell B., 2000, *ApJS*, 128, 615
- Mattila S., Lundqvist P., Sollerman J. et al., 2005, *A&A*, 443, 649
- Maguire, K., Taubenberger, S., Sullivan, M., Mazzali, P.A., 2016, *MNRAS*, 457, 3254
- Margutti, R., Soderberg, A. M., Chomiuk, L., et al. 2012, *ApJ*, 751, 134
- Margutti, R., Parrent, J., Kamble, A., et al. 2014, *ApJ*, 790, 52
- Marion, G. H., Brown, P. J., Vinkó, J. et al., 2016, *ApJ*, 820, 92
- McCully, C., Jha, S. W., Foley, R. J. et al., 2014, *Nature*, 512, 54
- Meng X., Chen X., Han Z., 2007, *PASJ*, 59, 835
- Meng X., Chen X., Han Z., 2008, *A&A*, 487, 625
- Meng, X., Chen, X., Han, Z., 2009, *MNRAS*, 395, 2103
- Meng, X., Yang, W., 2010, *A&A*, 516, A47
- Meng X., Yang W., 2011, *ScChG*, 54, 2296
- Meng, X. & Ph. Podsiadlowski, 2013, *ApJL*, 778, L35
- Meng, X. & Ph. Podsiadlowski, 2014, *ApJL*, 789, L45
- Meng X., Gao Y., Han Z., 2015, *IJMPD*, 24, 14, 1530029
- Meng, X., Han, Z., 2016, *A&A*, 588, A88
- Meng, X. & Podsiadlowski, Ph. 2017, *MNRAS*, 469, 4763
- Meng, X. & Podsiadlowski, Ph. 2018, *ApJ*, 861, 127, arXiv: 1801.00228
- Meng, X., & Han, Z., 2018, *ApJL*, 855, L18
- Miller G.E., Scalo J.M., 1979, *ApJS*, 41, 513
- Nomoto, K., Thielemann, F-K., Yokoi, K., 1984, *ApJ*, 286, 644
- Nomoto, K., Leung, S. 2018, *SSRv*, 214, 67
- Nugent, P. E., Sullivan, M., Cenko, S.B., et al., 2011, *Nature*, 480, 344
- Olling, R. P., Mushotzky, R., Shaya, E. J. et al., 2015, *Nature*, 521, 332
- Ostriker, J. P., & Bodenheimer, P., 1968, *ApJ*, 151, 1089
- Patat, E., Chandra, P., Chevalier, R., et al., 2007, *Science*, 317, 924
- Pakmor R., Röpke F.K., Weiss A., Hillebrandt W., 2008, *A&A*, 489, 943

- Pan, K., Ricker, P. M., Taam, R. E., 2012, *ApJ*, 750, 151
Pan, K., Ricker, P.M., Taam, R.E., 2014, *ApJ*, 792, 71
Podsiadlowski, P., 2003, arXiv: 0303660
Pérez-Torres, M. A., Lundqvist, P., Beswick, R. J. et al., 2014, 792, 38
Perlmutter, S., Aldering, G. Goldhaber, G. et al., 1999, *ApJ*, 517, 565
Pfannes, J. M. M., Niemeyer, J. C., & Schmidt, W. 2010a, *A&A*, 509, A75
Pfannes, J. M. M., Niemeyer, J. C., Schmidt, W., & Klingenberg, C. 2010b, *A&A*, 509, A74
Rho, J., Gomez, H. L., Boogert, A., et al., 2018, *MNRAS*, 479, 5101
Riess, A., Filippenko, A. V., Challis, P. et al., 1998, *AJ*, 116, 1009
Reimers, D. 1975, *Mem. R. Soc. liège*, 6ième Serie, 8, 369
Ruiz-Lapuente P. et al., 2004, *Nature*, 431, 1069
Ruiz-Lapuente, P., Damiani, F., Bedin, Luigi R., et al. 2018, *ApJ*, 862, 124, arXiv: 1711.00876
Saio, H., Nomoto, K., 2004, *ApJ*, 615, 444
Scalzo R., Aldering G., Antilogus P. et al., 2012, *ApJ*, 757, 12
Schaefer, B. E. & Pagnotta, A., 2012, *Nature*, 481, 164
Schweizer, F. & Middleditch, J., 1980, *ApJ*, 241, 1039
Shappee B. J., Stanek K. Z., 2011, *ApJ*, 733, 124
Shappee B. J., Stanek K. Z., Pogge R.W., Garnavich P. M., 2013, *ApJ*, 762, L5
Shappee, B.J., Piro, A.L., Stanek, K.Z., et al., 2018, *ApJ*, 855, 6
Silverman, J. M., Nugent, P. E., Gal-Yam, A. et al., 2013, *ApJS*, 207, 3
Shen, K. J., Guillochon, J., & Foley, R. J. 2013, *ApJ*, 770, L35
Shen, K. J., Boubert, D., Gänsicke, B.T., et al., 2018, *ApJ*, 865, 15
Taubenberger S., Kromer M., Hachinger S. et al., 2013, *MNRAS*, 432, 3117
Uchida, H., Yamaguchi, H., & Koyama, K. 2013, *ApJ*, 771, 56
Wang, B., Meng, X., Chen, X., Han, Z., 2009, *MNRAS*, 395, 847
Wang, B., Han, Z., 2009, *A&A*, 508, L27
Wang, B., Han, Z., 2012, *NewAR*, 56, 122
Wang, B., Justham, S., Liu, Z.-W. et al., 2014a, *MNRAS*, 445, 2340
Wang, B., Meng, X., Liu, D., Liu, Z., Han, Z., 2014b, *ApJL*, 794, L28
Webbink, R.F., 1984, *ApJ*, 277, 355
Whelan, J., Iben, I., 1973, *ApJ*, 186, 1007
Williams, B.J., Borkowski, K. J., et al., 2014, *ApJ*, 790, 139
Winkler, P. F., Gupta, G., Long, K.S., 2003, *ApJ*, 585, 324
Winkler, P. F., Long, K. S., Hamilton, A.J.S., Fesen, R.A., 2005, *ApJ*, 624, 189
Winkler, P. F., Hamilton, A. J. S., Long, K. S., & Fesen, R. A. 2011, *ApJ*, 742, 80
Worthey, G., Lee, H., 2011, *ApJS*, 193, 1
Wu, C.-C., Leventhal, M., Sarazin, C. L., & Gull, T. R. 1983, *ApJL*, 269, L5
Xiong, H., Chen, X., Podsiadlowski, Ph., Li, Y., Han, Z., 2017, *A&A*, 599, A54
Xue Z. & Schaefer B. E., 2015, *ApJ*, 809, 183
Yoon, S.-C., Langer, N., Scheithauer, S., 2004, *A&A*, 425, 217
Yoon, S.-C., Langer N., 2005, *A&A*, 435, 967
Zhou, P., Vink, J., 2018, *A&A*, 615, A150
Ziegerer, E., Heber, U., Geier, S., et al., 2017, *A&A*, 601, A58